SOVIET JOURNAL OF PARTICLES AND NUCLEI VOL. 3, NO. 2 OCTOBER-DECEMBER, 1972

THEORY OF NUCLEAR SHELL STRUCTURE. I

V. M. Kolomiets, B. D. Konstantinov,
V. M. Strutinsky, and V. I. Khvorost'yanov

Institute of Nuclear Research, Academy of Sciences of the Ukrainian SSR, Kiev
Translated from Fizika Élementarnykh Chastits i Atomnogo Yadra,
Vol. 3, No. 2, pp. 392-435, 1972

A shell correction model is formulated in order to describe oscillations of nuclear masses and other phenomena related to nucleon shells. In the theory, deviation of the actual nucleon distribution from the statistically averaged value plays the role of a small parameter. The relation between the shell oscillations of nuclear masses and shell structure effects in the spatial density distribution of nucleons is discussed.

1. INTRODUCTION

Observation of the shell structure of nuclei was of great significance in the development of nuclear physics, and it is quite natural that this phenomenon has attracted a great deal of attention. However, until recently a quantitative theory of shell structure had hardly been developed at all. Specifically, even a sufficiently clear qualitative definition of the shell structure in nuclei was absent, and the very concept of a shell was used to denote very different phenomena ranging from individual one-particle states to large isolated groups of such states whose existence is associated with the phenomenon of the magic nature of nuclei. Most frequently, degenerate j levels in the spherical average field of a nucleus [1] are called nucleon shells.

In contrast to this, we shall understand a shell to mean a large isolated group of nucleon levels (a large shell). The distance between the centers of gravity of such groups in the spectrum of one-particle states is characterized by energy intervals of the order of $\hbar\Omega = E_F/A^{1/3} = 6$-$8$ Mev (E_F is the Fermi energy). Correspondingly, the maximum number of nucleons in each group is $A^{2/3} = \hbar\Omega\bar{g}(E_F)$, where $\bar{g}$ is the average density of one-particle states:

$$\bar{g}(E_F) \approx A/E_F, \tag{1}$$

which is equal to 5-6 MeV^{-1} in a heavy nucleus. Hereafter we shall primarily be interested in phenomena associated with large shells. Effects associated with j levels of spherical nuclei or with some other similar structure having a smaller scale are also taken into account, although they have secondary significance.

Many important phenomena such as the existence of deformed nuclei, oscillations of the binding energy (masses) of the nuclei, etc., are associated with shells in nuclei. Suggestions have been made concerning the possible effect of shells on nuclear processes associated with considerable deformation of nuclei (fission) [2], but a quantitative theory of such phenomena, as well as rigorous qualitative definitions, has been absent. The theory of such phenomena was confined to results obtained by means of the little-substantiated method of summing one-particle energies in the deformed average potential [3, 4], by means of semiquantitative models that accentuate the role played by the residual interaction [5], or by means of purely phenomenological models. The latter particularly were used to describe the masses of nuclei and the theory of fission [6-9].

Among the phenomenological models one should note the Swiatecki–Myers model [6, 7], in which the oscillations of the masses and the deformation energies of the nuclei are identified with the oscillating part of the sum of the one-particle energies and the Weizsäcker equation is augmented by the appropriate correction term that takes this phenomenon into account phenomenologically.

Notwithstanding its success in describing known nuclear masses with a smaller number of param-

eters, such a phenomenological model does not solve the problem. Moreover, like other models based on the consideration of certain features of the one-particle spectrum, this model also does not provide an answer to the question of the significance of the shell fluctuations of nucleon interaction energy, which have a value of the same order as the energy variation of the one-particle levels.

A possible way of constructing a quantitative theory of shell phenomena has been noted in the so-called shell-correction method. This approach is based on the assumption that shell oscillations of the binding energy of nuclei and of the one-particle spectrum are associated with oscillations of the spatial density of the nucleons. The possibility of a special perturbation theory for the nuclear energy, in which deviations of the spatial distribution of the nucleons $\delta\rho$ from the smooth phenomenological background have small values, was noted in [10-12]. It turns out that in the first approximation in $\delta\rho$ the oscillations of the binding energy of nuclei actually do coincide with the oscillating part of the sum of the one-particle energies of the shell model, the result in this approximation being independent of the specific interactions between nucleons [10].

Pairing interaction of nucleons is important only for terms of second order in $\delta\rho$, which, in accordance with formal estimates given below, are $A^{1/3}$ times smaller than the principal term (i.e., than the shell correction). Pairing of nucleons likewise has a secondary significance. Eliminating secondary effects of the j-level degeneracy type, pairing merely emphasizes the effect of the shell structure. In quantitative calculations pairing of nucleons is taken into account conventionally.

As will be shown, only that portion of the density fluctuations which is due to the finiteness of the nuclear dimensions is associated with shell effects. Such oscillations evidently correspond to periodic classical trajectories of a particle in the potential well of a nucleus. In a system of noninteracting particles other density oscillations are also possible, and the question of a unique separation of these effects naturally develops. The problem of the nature of oscillations of the nucleon density in nuclei has great significance for calculations of the shell structure, and maximum attention will be devoted to it.

The principal assumptions on which the calculations of shell corrections are based do not depend on the form of the average nuclear field, and all those results that are described below apply equally to deformed nuclei. In the present paper calculations are given for spherical nuclei in which the Woods–Saxon potential of the shell model is used, while in the second part of the paper we shall consider the cases of deformed nuclei and applications to fission theory. A portion of the results expounded in the present paper was obtained during the stay of one of the present authors (V. M. Strutinsky) at the Niels Bohr Institute in Copenhagen and is included in the review paper [13].

2. THE SHELL MODEL AND SELF-CONSISTENT THEORY

Let us begin our consideration with the description of arguments based on the Hartree–Fock approximation. Within the framework of this simple approximation the principal concepts associated with the shell structure of nuclei are formulated, statistically averaged quantities are introduced, and equations are derived for the quantities characterizing the deviation of the true values from the average values. The results obtained are generalized in the theory of finite Fermi systems. A separate paper [14] is devoted to this, in which a detailed study has been made of the various improvements of the theory, including the generalization advanced by Bethe [15] of the shell-correction model for the case of the approximation of the Hartree–Fock type with a phenomenological interaction that depends on the local nucleon density [16]. Such refinements are not essential for the principal term in the shell-correction model approximation, which is the approximation that we shall consider here.

In the Hartree–Fock approximation the total energy of the system has the form

$$\mathcal{E}^{c} = \sum_{\lambda} n_{\lambda} E_{\lambda}^{c} - \frac{1}{2} \mathrm{Tr}\,(\rho^{c} v\,(1 - \mathcal{P})\,\rho^{c}), \qquad (2)$$

where $\mathcal{P}$ is the exchange operator; n_λ is the occupancy number; E_λ^c and Φ_λ^c are the one-particle energies and functions; ρ^c (1, 2) is the density matrix; v is the pairing interaction of the nucleons. The wave functions Φ_λ^c satisfy the Schrödinger equation

$$-\frac{\hbar^2}{2m}\Delta\Phi_\lambda^c(x) + V_L^c(x)\,\Phi_\lambda^c(x) - \int V_{NL}^c(x, x')\,\Phi_\lambda^c(x')\,dx' = E_\lambda^c \Phi_\lambda^c(x), \qquad (3)$$

where the local potential is

$$V_L^c(x) = \int dx' v(x, x')\,\rho^c(x', x'), \qquad (4)$$

the nonlocal potential is

$$V_{NL}^c(x, x') = v(x, x')\,\rho^c(x', x'), \qquad (5)$$

and the density matrix is

$$\rho^c(x, x') = \Sigma_\lambda n_\lambda \Phi_\lambda^{c*}(x)\,\Phi_\lambda^c(x'). \quad (6)$$

The subsequent conclusions are also valid if the two-particle interaction is different in the direct and exchange terms. The subscript c denotes the fact that the corresponding quantity is self-consistent.

In a system with finite dimensions, such as a nucleus, all self-consistent quantities included in Eqs. (2)-(6) [$\Sigma_\lambda E_\lambda n_\lambda$, ρ^c (x, x'), V^c] contain a component that oscillates from nucleus to nucleus or for a change in nuclear shape, along with a monotonic variation. The concept of the shape of the nucleus is defined in Sec. 5 and also in [13]. Our purpose consists in isolating the oscillating parts from the smooth background, which is many times greater. For this purpose let us introduce the smoothly varying quantity $\bar{\rho}$ (1, 2), which may be defined as the statistical average value of ρ^c (1, 2) over many nuclei or over many states of the same nucleus. Let us consider the average field $\bar{V} = \bar{V}_L + \bar{V}_{NL}$ that is defined by means of $\bar{\rho}$ using the same relationships as those used for the self-consistent field:

$$\bar{V} = \int dx v(x, x')\,\bar{\rho}(x', x') - [v(x, x')\,\rho(x', x')]_{\text{nonlocal}}. \quad (7)$$

It is obvious that $\bar{V}$ is also a smooth quantity. This allows us, at least in principle, to identify $\bar{V}$ with the phenomenological potential V^S of the shell model, which, like $\bar{V}$, is not a self-consistent quantity and according to the principal assumption of the shell model varies smoothly from nucleus to nucleus. The irregular variations that are characteristic of the true self-consistent average field are completely ignored in V^S, just as they are in $\bar{V}$.

Note that in the traditional shell model the phenomenological average field V^S is introduced immediately in place of $\bar{\rho}$. This fact does not alter the essence of the situation, since it may be assumed that V^S takes into account all terms that develop in $\bar{V}$ (for example, the exchanging part). In what follows, this imperfection of the practical shell model does not have great significance, since all of the results are determined by a comparatively narrow band near the Fermi energy, where the corrections are negligible.

Solving the one-particle problem of the shell model with an average field $\bar{V}$, we find the one-particle states Φ_λ^S and E_λ^S. Their relationships may be conventionally depicted in the following form:

$$\rho(x, x') \to \bar{V}(x, x') \to E_\lambda^s,\ \Phi_\lambda^s \to \rho^s(x, x') \quad (8)$$

for the shell model and

$$\rho^c(x, x') \to V^c(x, x') \to E_\lambda^c,\ \Phi_\lambda^c \to \quad (9)$$

for the self-consistent quantities. It is clear that the density matrix of the shell model

$$\rho^s(x, x') = \Sigma_\lambda n_\lambda \Phi_\lambda^{s*}(x)\,\Phi_\lambda^s(x') \quad (10)$$

does not coincide either with $\bar{\rho}$ or with ρ^c. As is the case with ρ^c, ρ^S is not a smooth quantity. Let us now assume that $\bar{\rho}$ differs little from ρ^c:

$$\rho^c = \bar{\rho} + \delta\rho, \quad (11)$$

where

$$|\delta\rho| \ll |\bar{\rho}|,\ |\rho^c|.$$

The difference between the self-consistent and average potentials

$$\delta V = V^c - \bar{V}$$

can be expressed in terms of $\delta\rho$ by means of Eq. (7). Treating the quantity δV as a small external perturbation, one may represent the difference between the self-consistent quantities and the solutions of the problem with a smooth but nonself-consistent potential in the form of a perturbation-theory series:

$$\mathscr{E}_\lambda^c = \mathscr{E}_\lambda^s + \int d1 \Phi_\lambda^{s*} \delta V \Phi_\lambda^s + \Sigma_{\lambda' \neq \lambda} |(\delta V)_{\lambda\lambda'}|^2/(E_\lambda - E'_\lambda), \quad (12)$$

$$\rho^c = \rho^s + \delta_1\rho, \quad (13)$$

where

$$\delta_1\rho = \Sigma_{\lambda\mu} \frac{n_\lambda - n_\mu}{E_\lambda - E_\mu} (\delta V)_{\lambda\mu} \Phi_\lambda^*(1)\,\Phi_\mu(2). \quad (14)$$

Substituting Eqs. (12) and (14) into Eq. (2) for the total energy and making use of Eq. (13), we find that with an accuracy to terms of the third order in $\delta\rho$ we have

$$\mathscr{E}^c = \mathscr{E}_0 + I, \quad (15)$$

where I contains terms which are of order no lower than the second in $\delta\rho$, and

$$\mathscr{E}_0 = \Sigma_\lambda E_\lambda^s n_\lambda - \frac{1}{2} \mathrm{Tr}\,[\bar{\rho} v (1 - \mathscr{P}) \bar{\rho}]. \quad (16)$$

The second-order term in (15) is

$$I = -\frac{1}{2} \int\int d1\, d2 v(1, 2)\,[\delta_1\rho(1)\,\delta\rho(2) - \delta_1\rho(1, 2)\,\delta\rho(1, 2)] +$$

$$+\frac{1}{2}\int\int d1\,d2 v(1,2)\,[\delta\rho(1)\,\delta\rho(2)-|\delta\rho(1,2)|^2], \quad (17)$$

and here and further on we use the identity

$$\rho(1)\equiv\rho(1,1).$$

Note now that in accordance with the definition of $\overline{\rho}^c$ and $\overline{V}$ the average value is given by

$$\overline{\delta V}=0. \quad (18)$$

Hence it follows that with an accuracy to quantities of second order in $\delta\rho$ we have

$$\overline{\rho}^c=\overline{\rho}^s. \quad (19)$$

From this equation and from (13) we obtain

$$\delta\rho=\rho^c-\overline{\rho}^c\approx\delta\rho^s+\delta_1\rho, \quad (20)$$

where $\delta\rho^s=\rho^s-\overline{\rho^s}$. In the representation of eigenfunctions of the shell model Eq. (20) has the form

$$\delta\rho_{\lambda\lambda'}=\delta\rho^s_{\lambda\lambda'}+\frac{n_\lambda-n_{\lambda'}}{E_\lambda-E_{\lambda'}}(\delta V)_{\lambda\lambda'}. \quad (21)$$

Since δV and $\delta\rho$ are linearly related, the latter expression may be treated as an integral equation for $\delta\rho$:

$$\delta\rho_{\lambda\lambda'}=\delta\rho^s_{\lambda\lambda'}+\frac{n_\lambda-n_{\lambda'}}{E_\lambda-E_{\lambda'}}\sum_{\alpha\beta}\langle\lambda\lambda'|v(1-\mathcal{P})|\alpha\beta\rangle\,\delta\rho_{\alpha\beta}. \quad (22)$$

Let us now introduce the scattering amplitude Γ in the medium, which satisfies the equation [17]

$$\langle\lambda\mu|\Gamma|\lambda'\mu'\rangle=\langle\lambda\mu|v(1-\mathcal{P})|\lambda'\mu'\rangle$$
$$+\sum_{\alpha,\alpha'}\langle\lambda\alpha|v(1-\mathcal{P})|\lambda'\alpha'\rangle\frac{n_\alpha-n_{\alpha'}}{E_\alpha-E_{\alpha'}}\langle\alpha\mu|\Gamma|\alpha'\mu'\rangle. \quad (23)$$

Using Γ, one can express $\delta\rho$ directly in terms of $\delta\rho^s$:

$$\delta\rho_{\lambda\lambda'}=\delta\rho^s_{\lambda\lambda'}+\sum_{\alpha\beta}\frac{n_\lambda-n_{\lambda'}}{E_\lambda-E_{\lambda'}}\langle\lambda\lambda'|\Gamma|\alpha\beta\rangle\,\delta\rho^s_{\alpha\beta}. \quad (24)$$

Having made use of this, we write

$$I=1/2\int\int d1\,d2\,\delta\rho^s\Gamma\delta\rho^s$$
$$=1/2\sum_{\lambda\mu\lambda'\mu'}\langle\lambda\mu|\Gamma|\lambda'\mu'\rangle\,\delta\rho^s_{\lambda\lambda'}\delta\rho^s_{\mu\mu'}. \quad (25)$$

Thus, the difference between the exact expression (2) for the self-consistent energy and the approximate expression (16) is of the second order in $\delta\rho$, and it is with this accuracy that one can use the second, considerably simpler expression for the energy, which does not require solution of the self-consistent problem.

As will be shown below, the average amplitude of the shell oscillations $\delta\rho$ is actually very small—of the order of $A^{-2/3}$ or less—and therefore the first approximation in Eq. (16) would already have comparatively good accuracy. However, in order to use it practically it would be necessary to define and calculate the quantities included there very precisely. This is hardly possible: Each of the components of Eq. (16) is a quantity of the order of 10^3 MeV, and it is clear that even a small physical or numerical discrepancy could lead to too large an error. Therefore, the calculation of the energy by means of the approximate equation (16) is almost as difficult as finding the self-consistent solution, all of the shortcomings of the original Hartree–Fock approximation being preserved.

Hereafter we shall be interested only in the oscillating part of the binding energy of the nucleus, and in such a case Eq. (16) has considerable advantages. Unlike Eq. (2), in which both terms oscillate, in (16) the shell oscillations are completely transferred to a comparatively simple term: Namely, they are contained in the sum of the one-particle energies that are calculated for the smooth nonself-consistent potential of the shell model. The second term in (16) is by definition a smooth quantity. Thus, in the first approximation in $\delta\rho$ the shell variations of the binding energy coincide with the variation of the one-particle energy alone.

The specific method of isolating the oscillations of the one-particle energy is described in the next chapter. It turns out that the energy oscillations are determined chiefly by certain features of the energy distribution of the one-particle levels near the Fermi energy in an interval that is fairly broad but at the same time small in comparison to the magnitude of the Fermi energy. This fact is of great significance, since it is well known that the approximation of independent particles having a relatively weak residual interaction is actually valid in this case [17]. Deeper states yield a contribution to the smooth parts. However, such terms can be replaced by a phenomenological expression: the Weizsäcker equation or the drop model. As a result, the independent-particle (or quasiparticle) approximation is used only to calculate the energy oscillations, which are determined by the region near the Fermi energy where such an approximation is justified.

The result of the first approximation of the shell-correction model may be improved by taking into account the second-order terms in Eq. (16). These corrections depend on the residual interaction. Their generalization in the Fermi-liquid model does not present any difficulties. Actually, Eqs. (23)-(25) are the characteristic equations of the Fermi-liquid theory. As will be shown below, the principal term of the shell correction may also be written in a form characteristic of the Fermi-liquid theory.

Normalization of the energy to the phenomenological Weizsäcker equation requires a definite compatibility with the drop model: The isolated oscillating pieces must not contain terms that are already included in the drop model (such as, for example, the volume or surface energy). Further, the answer must not depend on the parameters which it is necessary to introduce in calculating the average values.

The requirement of uniqueness should not be understood too literally. A certain indefiniteness in finding the smooth quantities may lead to a situation in which the isolated oscillations also contain a small smooth component. It is clear that the presence of a component that varies smoothly by several megaelectron volts for a substantial difference in the atomic weight or shape of the nucleus does not have significance at this stage and does not affect the comparison with experiments. However, the requirement of even this accuracy puts forward nontrivial conditions. This problem will be considered in greater detail below.

In conclusion, note that Eq. (16) to some measure justifies the method advanced by Mottelson and Nilsson [3] for calculating equilibrium deformations of nuclei as the minima of the sums of one-particle energies that have been determined for the shell potential of the Nilsson model. As is well known, such a method is used quite successfully to calculate the quadrupole moment of nuclei in ground states, which may be explained by the fact that for small quadrupole deformations the change of the smooth part of the energy (16) has practically no effect on the position of the minimum of the deformation energy. The Mottelson–Nilsson method, however, is totally unsuitable for more complex or larger quadrupole deformations; this may easily be explained by means of Eq. (16). The Mottelson–Nilsson method has been criticized frequently because of the fact that supposedly it does not take into account variations in the average energy of nucleon interaction, whose amplitude is comparable with the variations of the one-particle energy. This criticism was based on Eq. (2) for the total energy, which had little relation to what was actually done. Actually, in such calculations the sum of the one-particle energies found for the smooth shell potential was always considered, and this corresponds to Eq. (16) rather than to self-consistent one-particle energies as is the case in Eq. (2). There is a certain difference between these two sets of energies, which becomes substantial in summation over many nucleon states. Note that for this same reason the method of determining the parameters of the shell potential as an effective potential well for many nuclei from a comparison with the experimentally observed energies of the one-particle levels in some isolated nucleus is not completely justified. The phenomenological potential found in this manner would be suitable for describing a specific situation in a specific nucleus, while it is necessary to find the effective smooth potential, which is the best approximation for many nuclei, from the interpretation of the shell model.

3. OSCILLATIONS OF THE TOTAL ONE-PARTICLE ENERGY

As is evident from Eq. (12), in order to isolate the oscillations of the binding energy of a nucleus in the first approximation in $\delta\rho$ it is sufficient to consider the total sum of the one-particle energies E_λ^s calculated for the appropriate smooth potential $\bar{V}$:

$$\mathcal{U} = 2\Sigma_\lambda n_\lambda E_\lambda. \tag{26}$$

Here and below we have introduced a factor arising as the result of summation over the spin, and the subscript s for quantities applying to the shell model has been dropped. Using $\tilde{\mathcal{U}}$ to denote the smooth component of the quantity $\mathcal{U}$, we write the oscillating part in the form

$$\delta\mathcal{U} = \mathcal{U} - \tilde{\mathcal{U}}. \tag{27}$$

The energy of the system is

$$\mathcal{E} \approx \mathcal{E}_0 + 0[(\delta\rho)^2] \approx \tilde{\mathcal{E}} + \delta\mathcal{U}, \tag{28}$$

where

$$\tilde{\mathcal{E}} = \tilde{\mathcal{U}} - \frac{1}{2}\mathrm{Tr}(\bar{\rho}v(1-\mathcal{P})\bar{\rho}). \tag{29}$$

This quantity is the analog of the expression for the total energy in the statistical models based on the Thomas–Fermi approximation. It may be replaced by the phenomenological liquid-drop expression for the nuclear mass, which is the best smooth approxi-

mation of nuclear masses (the Weizsäcker equation). Thus, the nuclear mass is represented in the form

$$M(N, Z, \text{shape}) = M_{\text{D.M.}} + \Sigma_{p,n}(\delta\mathcal{U} + P),$$

where $M_{D.M}$ is the conventional liquid-drop expression for the mass; the sum is taken over protons and neutrons. In Eq. (30) the term P corresponding to the pairing correlation energy has also been added. In particular this term takes into account the considerable variations of pairing energy which are associated with the variation of the density of one-particle states near the Fermi energy (i.e., with the energy shells). Even–odd variations of the pairing energy are usually included in the phenomenological-drop part.

The nuclear deformation is also indicated as an external parameter in Eq. (30), since all the quantities in Eq. (30) are determined for a given shape of the nuclear surface. The representation of the energy in the form (30) is especially convenient, since it is precisely this representation that is adopted in the phenomenological description of nuclear masses. Consequently, the calculated magnitude of the shell correction may be compared directly with the experimental value of the deviations of the nuclear masses from the best smooth liquid-drop approximation. Considering the energy variation as a function of the nuclear shape, we obtain the deformation energy, the second term in Eq. (30) representing the shell variations of the deformation energy relative to the average drop value. The extrema of the deformation energy correspond to stationary shapes of the nuclear surface: The minima correspond to the stable states, while the maxima or saddle points correspond to thresholds of the deformation energy. Thus, one may calculate the shape of the nucleus in the ground state (the lowest minimum), after which one may calculate the correction to the binding energy of the ground state (see Sec. 6).

The shell oscillations of the nuclear masses, which are treated as functions of the atomic number, can be characterized by a period of the order of $A^{2/3}$. Therefore, the smooth one-particle energy can be obtained if one considers quantities which have been averaged with respect to the one-particle spectrum over an interval of the order of[1]

$$\tilde{\gamma} \approx \hbar\Omega = E_F/A^{1/3} \approx 5\text{-}10 \text{ MeV},$$

containing $A^{2/3}$ or more particles. For isolation of the shell oscillations of the energy the density of one-particle states averaged over the interval γ, which is equal to

$$\tilde{g}(E) = g_{\tilde{\gamma}}(E),$$

is of principal significance, where g_γ is determined by the expression

$$g_\gamma(E) = 1/\gamma\Sigma_\lambda f[(E_\lambda - E)/\gamma]. \quad (31)$$

The weighting function $f(x)$ is of the order of unity if $|x| \lesssim 1$, and vanishes outside this interval. It is convenient to choose this function to have the following form:

$$f(x) = \frac{1}{\sqrt{\pi}} \exp(-x^2) P_{2m}(x). \quad (32)$$

This expression contains an arbitrary weighting factor P_{2m}, which is permitted since the smoothness condition alone still does not determine the function $\tilde{g}(E)$ uniquely. The specific form of P_{2m} follows from additional physical conditions. Here we note only that the correcting function (polynomial) $P_{2m}(x)$ also must be of the order of unity for $|x| \lesssim 1$. The smoothed one-particle energy $\tilde{\mathcal{U}}$ in Eq. (27) is determined by the density $\tilde{g}(E)$ according to

$$\tilde{\mathcal{U}} = 2\int_{-\infty}^{\tilde{E}_F} Eg(E)\,dE, \quad (33)$$

where the limiting energy for the uniform distribution E_F is found from the condition of conservation of the number of particles:

$$N = 2\int_{-\infty}^{\tilde{E}} g(E)\,dE. \quad (34)$$

Thus, the principal term of the shell correction is

$$\delta\mathcal{U} = 2\Sigma_\lambda n_\lambda E_\lambda - 2\int_{-\infty}^{\tilde{E}_F} Eg(E)\,dE. \quad (35)$$

The shell correction $\delta\mathcal{U}$ is completely determined by the one-particle energy spectrum of the shell model and can easily be calculated by means of Eqs. (34) and (35) for any given distribution of the one-particle levels. The amplitude $\delta\mathcal{U}$ is determined by the deviation of the actual level distribution from

[1] In those equations in which the absolute value of the Fermi energy is taken into account, we have in mind E_F measured from the bottom of the well (i.e., the average kinetic energy of the nucleons).

the smooth distribution characterized by the average density $\tilde{g}$. For qualitative discussions it is convenient to introduce a certain local density of the one-particle states g_s (E) along with the average density $\tilde{g}$; this local density may also be determined by means of Eq. (31) after taking a $\tilde{\gamma} = \gamma_s$ that is small compared with $\tilde{\gamma}$ as the averaging interval. The quantity

$$\delta g(E) = g_s(E) - \tilde{g}(E) \tag{36}$$

represents the deviation of the local density of the levels from the average value for the energy E obtained by averaging over a broad interval $\tilde{\gamma}$. Using g_s, one can write $\delta\mathcal{U}$ in the form

$$\delta\mathcal{U} \approx 2\left\{\int_{-\infty}^{E_F} Eg_s(E)\,dE - \int_{-\infty}^{\tilde{E}_F} E\tilde{g}(E)\,dE\right\} \tag{37}$$

$$\approx 2\int_{-\infty}^{E_F} (E - E_F)\,\delta g(E)\,dE. \tag{38}$$

This expression is stationary relative to small variations of the boundary energy, and consequently the two Fermi energies are assumed to be identical here. Another useful expression for the shell correction without the occupancy number will be derived below.

Expression (38) for the shell correction establishes a connection between the variations of the nuclear masses and the shells in the one-particle spectrum. It may be used for specific calculations. Under these conditions the parameter γ_s is taken equal to 1-2 MeV. In accordance with the quasiclassical estimate such an interval contains an average of five to six levels, and, at first glance, the local density g_s(E) must also be a smooth function of the one-particle energy and differ little from $\tilde{g}$ (E). Actually, g_s oscillates strongly about an average value equal to $\tilde{g}$, the same thing occurring in deformed nuclei also. The minima of g_s correspond to the magic regions of rarefied levels in the one-particle spectrum ("filled shells"), and here $\delta g < 0$. In practice the value of g_s varies by a factor of severalfold for a transition from the middle of the shell to a filled shell (Fig. 1) in any one-particle model and independently of the shape of the nucleus. It is necessary to emphasize the fact that in the presence of shell groupings of levels no unique value exists for g_s, even though the interval γ_s contains a good many levels. Such a fact does not have great significance, since only those intervals of g_s have meaning for which limiting values equal to the exact sums over the one-particle spectrum exist even for $\gamma_s \to 0$.

The condition for independence of $\tilde{g}$ (E) from the specific value of the parameter $\tilde{\gamma}$ is more es-

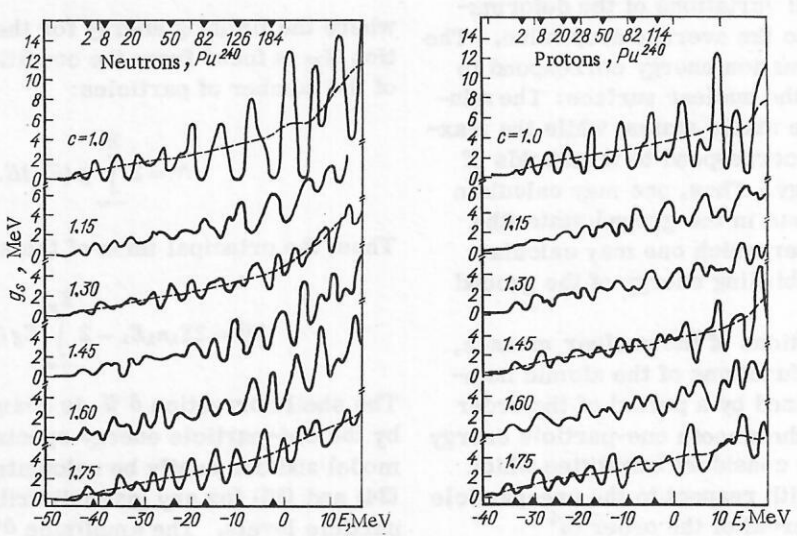

Fig. 1. Density of one-particle levels in spherical and deformed Woods–Saxon potentials for the Pu^{240} nucleus: The solid curves are for the local density obtained for averaging with γ^s = 1.5 MeV; the dashed lines are for the smoothed level density ($\tilde{\gamma}$ = 8 MeV). The shape of the potential well corresponds approximately to the sequence of nuclear shapes in the fission process; the values of the deformation parameter of a well equal to the ratio between the major semiaxis of the nucleus and the radius of a sphere of equal size [13] are indicated next to the curves.

sential and considerably less trivial. In the final analysis according to (33) it is this condition which determines the uniqueness of the isolation of the energy oscillations. The smoothed one-particle energy $\tilde{\mathcal{U}}$, and along with it $\delta\mathcal{U}$, as a function of $\tilde{\gamma}$ must have a fairly broad plateau, and must remain constant with an accuracy of the order of 10^{-4} in the region of the plateau if we are speaking of calculating shell corrections with an accuracy of the order of several hundred keV.

Meanwhile the simple intuitive procedure for calculating the average value of the level density—the number of levels in the interval is calculated and divided by the size of the interval for a finite γ—is not unique. The uncertainty of the order of $E_F\gamma^2(d^2\tilde{g}/dE^2) \approx (\gamma/E_F)$ that develops is small, but it has exceptional significance for the calculation of $\delta\mathcal{U}$. Let us recall that the corrections to $\mathcal{U}$ corresponding to the one-particle surface energy [12] have precisely such an order of smallness. Therefore a condition also develops for determining the smooth quantities, that the shell correction $\delta\mathcal{U}$ must not contain smooth dependences on the external parameters, which are similar to those included in the drop portion of the phenomenological Weizsäcker equation (such as the volume and surface energy). Otherwise such terms would be taken into account twice, and the entire procedure described above would lose its meaning. In order for $\delta\mathcal{U}$ not to contain components similar to the principal terms of the drop energy it is necessary to retain the smooth terms in the smoothed one-particle energy $\tilde{\mathcal{U}}$ during the averaging process, which are the same as those in the sum of the shell one-particle energies, i.e., they must vanish in the difference between these quantities in Eq. (27). This condition actually coincides with the requirement that the averaged quantity coincide with the exact local value of the density in the case of a uniform distribution. From this we find the weighting function P_{2m} in (32), which so far has remained undetermined. Let us require that a quantity averaged over a finite interval γ coincide with the exact local value at the point E for a uniform distribution of the levels, which may be described by a polynomial with degree no higher than 2m.

From this condition we find P_{2m} in the form of a polynomial of degree 2m in $x = (E - E')/\gamma$, the coefficient of this polynomial being associated in a definite way with the even derivatives of $\tilde{g}$ of increasing order; it also can be shown that the expansion in the small parameter $(\gamma/E_F)^2$ holds [12]. It has been noted [18, 29] that in using a Gaussian weighting function in (31) the correcting polynomial is the sum of the first m terms of the expansion of a δ function in a series in Hermite polynomials. This allows the following general expression to be obtained for the correcting polynomial of degree 2m:

$$P_{2m} = \sum_{k=0,2,\ldots}^{2m} \alpha_k H_k(x). \tag{39}$$

The coefficients α_k are determined from the recursion relations

$$\alpha_k = -\frac{1}{2_k}\alpha_{k-2},\ \alpha_0 = 1.\Big\} \tag{40}$$

The degree of the correcting polynomial is chosen from the following condition: For all averaged quantities the plateau region with a maximum width should be obtained as a function of the parameter $\tilde{\gamma}$. The degree of the correcting polynomial must not be too high, or the condition requiring smoothness of the smooth quantity will be violated. This condition yields a maximum value of the order of $\overline{E}_F/\tilde{\gamma} \approx A^{1/3}$ for 2m. The check of the correctness of the choice of the correcting function resides in the fact that in the region of the plateau the quantity $\delta\mathcal{U}$ must remain constant as the degree of the correcting polynomial changes. Usually, 2m = 4 or 6 is used.

Numerous specific calculations [12, 13, 18] have confirmed that in this manner one can achieve fulfillment of all the conditions enumerated above. The exclusion from $\delta\mathcal{U}$ of the component proportional to the surface is confirmed by the fact that the calculated shell corrections oscillate near the zero value either with inclusion of the dependence on the size of the nucleus (or on the atomic number) for a given shape, or for a change in the nuclear shape.

The condition for the existence of a plateau and for uniqueness of the results for different choices of the correcting polynomial is fulfilled best in those cases when the levels are distributed fairly uniformly (as, for example, in a harmonic oscillator) and the one-particle states are known in a fairly large interval near the Fermi energy (of the order of 2 to 4 $\hbar\Omega$). In calculations with a potential having a finite depth (the Woods–Saxon model) a natural difficulty develops which is associated with the fact that the Fermi energy is situated too close to the edge of the potential well and the number of discrete states above the Fermi energy is insufficient for application of the averaging procedure with large γ. In this case the region of the

plateau may be isolated by carrying out calculations with a potential well having a large radius, so that the Fermi energy descends sufficiently low. The quantity $\delta\mathcal{U}$ calculated in this manner can then be extrapolated to the "correct" radius of the well. Monitoring calculations show that the correct values of $\delta\mathcal{U}$ can also be obtained in calculations with a conventional potential of the Woods–Saxon model, provided that a $\bar{\gamma}$ = 5–6 MeV is chosen that is not too large, even in those cases when no plateau is obtained for a further increase in $\bar{\gamma}$.

Examples of the saturation of $\delta\mathcal{U}$ as a function of $\tilde{\gamma}$, which applies to the Woods–Saxon model, the Nilsson model, and the spherical harmonic-oscillator model, are shown in Fig. 2. In the Woods–Saxon potential only the levels of the discrete spectrum were taken into account, while the radius was taken to be somewhat larger than the normal value. The curves are shown for various degrees 2m of the correcting polynomials. The plateau region is clearly visible. Without the correcting polynomial a meaningless result is obtained, which corresponds to "heating" of the nucleus to a "temperature" of the order of γ.

Specific difficulties in calculations with the Woods–Saxon potential may also be avoided if one uses all the levels above the Fermi energy which are obtained by diagonalizing the Hamiltonian on a limited basis with spatial dimensions that are approximately equal to the dimensions of the nucleus [19]. Such a diagonalization, together with the true discrete states, yields states having positive energies which are fully usable for extrapolation of the one-particle spectrum. Under specified conditions these states are close to the corresponding quasistationary one-particle levels. In order to spread the spectrum it is not at all mandatory to use the exact quasistationary levels of the continuum. In the averaging process the high states are required to the extent to which they approximate the discrete spectrum of heavier nuclei in the region of atomic weights of order $A^{2/3}$. Therefore the negative results found by Lin [20] with a very limited number of discrete levels near the Fermi energy and exact resonances of the continuum do not correspond to reality. Note, however, that in the Lin calculations values of shell corrections are also obtained at γ = 5–6 MeV that are close to those given by the Nilsson model or by the Woods–Saxon potential.

The problem of the contribution of various states to the shell fluctuations and the problem of the size of the minimal interval that yields saturation for the shell corrections will be considered in part II (see also [13]).

Let us present still another representation for shell corrections that is clear and convenient for practical calculations. By using it one can show that a substantial contribution to $\delta\mathcal{U}$ is actually made only by a relatively narrow layer of one-particle states of the order of $\tilde{\gamma}$ near the Fermi energy. For this purpose let us use the specific function

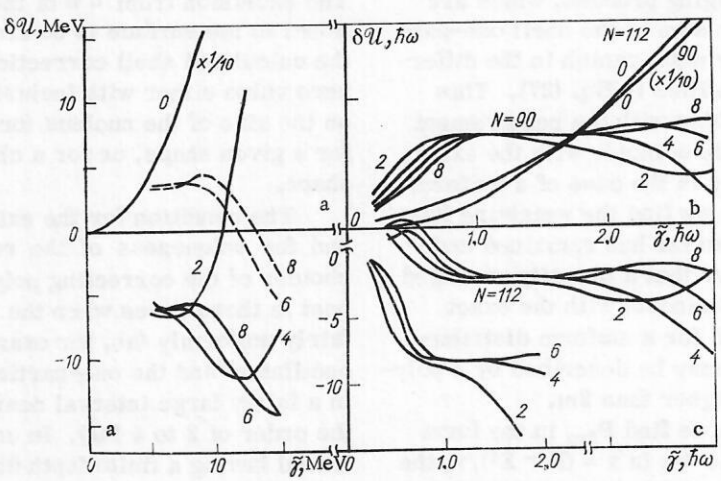

Fig. 2. Dependence of the shell correction $\delta\mathcal{U}$ on the parameter $\tilde{\gamma}$ for the Woods–Saxon model (a), for the spherical harmonic-oscillator model (b), and for the Nilsson model (c): a) the solid line is for N = 126, the dashed line is for N = 114; the degree 2m of the correcting polynomial is also shown next to each curve. The data for the Nilsson model have been taken from [18].

$\tilde{g}$ (E) in the form of a sum over the one-particle spectrum (31), and also Eq. (32) for the correction function $P_{2m}(x)$. After integration with respect to energy in Eq. (35) we obtain the following expression for the shell correction in the form of a sum over the one-particle spectrum:

$$\delta\mathcal{U} = 2\Sigma_\lambda E_\lambda \delta n_\lambda + \gamma^2 g^*(E_F). \quad (41)$$

Here

$$\delta n_\lambda = n_\lambda - \tilde{n}_\lambda \quad (42)$$

is the difference between the two distributions of the occupancy numbers; n_λ is the distribution of the ground state of the nucleus; $\tilde{n}_\lambda$ is a certain distribution which is spread about the Fermi energy by the amount $\tilde{\gamma}$:

$$\tilde{n}_\lambda = n(\varepsilon_\lambda) = \int_{\varepsilon_\lambda}^{\infty} f(x)\,dx, \quad (43)$$

where

$$\varepsilon_\lambda = (E_\lambda - \tilde{E}_F)/\tilde{\gamma}.$$

In Eq. (11) g*(F) corresponds to a certain effective density of the equations near the Fermi energy, which is calculated with a different weighting function than the one used in the case of the density $\tilde{g}$; therefore it differs from the latter:

$$g^*(E) = \frac{1}{\tilde{\gamma}} \Sigma_\lambda f^*[(E_\lambda - E)/\tilde{\gamma}], \quad (44)$$

where

$$f^*(x) = \alpha_{2m} H_{2m}(x) \exp(-x^2)/\sqrt{\pi}. \quad (45)$$

The two densities coincide if the correcting polynomial is absent (2m = 0). For n(x) the following expression is convenient:

$$n(x) = \frac{1}{\sqrt{\pi}} \exp(-x^2)\left[\Pi(x) + \sum_{k=2,4,\ldots}^{2m} \alpha_k H_{k-1}(x)\right]. \quad (46)$$

For the function

$$\Pi(x) = \exp(+x^2)\left[\sqrt{\pi} - \int_{-\infty}^{x} \exp(-t^2)\,dt\right]$$

for $x \geq 0$ one can use the following numerical approximation:

$$\Pi(x) = \Sigma_{i=1}^{5} b_i t^i,$$

where

$$t = 1/(1+px);$$

$$b_1 = 0.22583684; \quad b_4 = -1.28782245;$$
$$b_2 = 0.25212867; \quad b_5 = 0.94064607;$$
$$b_3 = 1.25969513; \quad p = 0.32759112.$$

For $x \leq 0$ one can use the identity

$$n(x) = 1 - n(-x).$$

The Fermi energy for the spread distribution is determined from the condition of conservation of the number of particles:

$$\delta N = 2\Sigma_\lambda \delta n_\lambda = 0. \quad (47)$$

Here it is assumed that the Fermi energy E_F for the real distribution is known. In the independent-particle model we have

$$n_\lambda = 1 - \theta(E_\lambda - E_F) = \begin{cases} 1, & E_\lambda < E_F; \\ 0, & E_\lambda \geq E_F. \end{cases}$$

In this case it is convenient to take E_F^0 in the form

$$E_F^0 = \frac{1}{2}(E_{\lambda<} + E_{\lambda>}),$$

where $E_{\lambda<}$ and $E_{\lambda>}$ are the energies of the last filled and first vacant levels, and to use this quantity as the initial value in the numerical procedure of searching for $\tilde{E}_F$. The shape of the distribution of δn is given in Fig. 3, the two limiting energies E_F and $\tilde{E}_F$ being assumed identical for simplicity. The quantity δn oscillates slightly for large values of the argument. This is reflected in an unusual behavior of the smoothed distribution of the occupancy numbers $\tilde{n}$, which sometimes turns out to be greater than unity or less than zero (Fig. 4).

Equations (41) and (43) in explicit form show that for the shell corrections only a limited interval

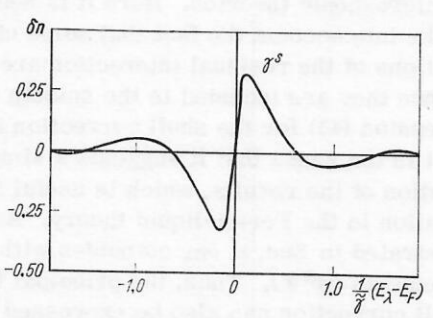

Fig. 3. Dependence of the distribution δn_λ for the correcting polynomial 2m = 4 on the level energy E_λ.

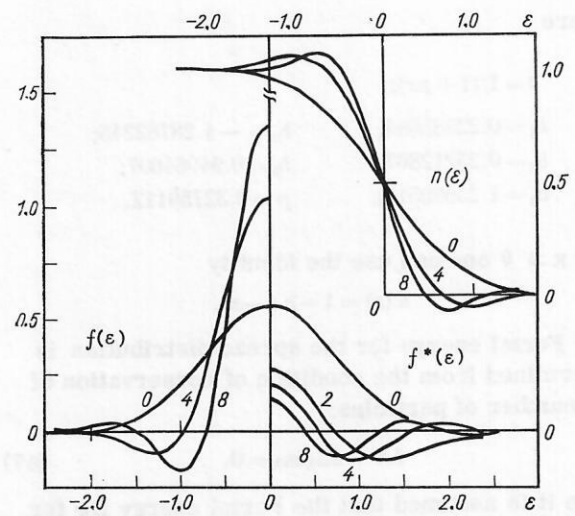

Fig. 4. Three universal functions for calculation of the shell corrections for various values of the degree 2m of the correcting polynomials as a function of the dimensionless argument ε.

of the order of $\gamma \approx E_F/A^{1/3}$ near the Fermi energy is of essential significance. The states that are distant from E_F by more than $2\text{-}3\tilde{\gamma}$ may be neglected entirely in the calculations. However, they are necessary to determine the Fermi energy of the actual distribution E_F if the position of E_F among the upper one-particle levels is not known either from any other considerations or directly from experimental data. This question has no relation to the actual shell-correction method. As has been noted above, in order to calculate the shell corrections one requires merely the one-particle states in a relatively narrow interval near the Fermi energy. It is also essential that the shell corrections are determined by the large-scale shell inhomogeneities, on which the residual interaction has relatively little effect. This does not interfere with inclusion of the residual interaction in quantitative calculations, which can be achieved in the existing microscopic theories. Here it is necessary to take into account the fact that some of the manifestations of the residual interaction are eliminated, since they are included in the smooth terms.

Expression (41) for the shell correction is also of interest in the sense that it suggests a simple interpretation of the results, which is useful for generalization in the Fermi-liquid theory. As will be demonstrated in Sec. 4, δn_λ coincides with the matrix elements $\delta\rho^S(r)$. Thus, the principal term of the shell correction can also be expressed in terms of this quantity, which characterizes the shell variations of the spatial distribution of the nucleons.

Note that the second term in Eq. (41) vanishes if the distribution of one-particle levels is sufficiently smooth and can be described by a polynomial of degree no higher than $2m-1$. This may be verified if in Eq. (44) the sum over the one-particle spectrum is replaced by an integral over energy and the orthogonality of the Hermite polynomials is taken into account. The formal estimate for the term is

$$\tilde{\gamma}^2 g^*(E_F) \approx \frac{\tilde{\gamma}^{2(m+1)}}{\sqrt{\pi}\,(2m)!}\alpha_{2m} g^{(2m)}(E_F)\int_{-\infty}^{\infty}\varepsilon^{2m}H_{2m}e^{-\varepsilon^2}\,d\varepsilon \approx \frac{(2m-1)!!}{2^m}\tilde{\gamma}^2\tilde{g}(E_F)\,(\tilde{\gamma}/(E_F)^{2m}, \tag{48}$$

where $\tilde{g}^{(2m)}-2m$ is the derivative of the smoothed level density. In numerical calculations the quantity $\gamma^2\tilde{g}^*(E_F)$ decreases abruptly in the region of the plateau in Fig. 2, taking on negligibly small values. Thus, for the shell correction one can use the simple expression

$$\delta\mathcal{U} = \Sigma_\lambda (E_\lambda - E_F)\ \delta n_\lambda, \tag{49}$$

where δn_λ are given by Eqs. (42) and (43). This corresponds to the smoothed one-particle energy

$$\tilde{\mathcal{U}} = 2\Sigma_\lambda E_\lambda \tilde{n}_\lambda,$$

which coincides with Eq. (33) for a correct choice of the parameter $\tilde{\gamma}$ that ensures sufficient smoothness of $\tilde{g}(E)$ near the Fermi energy. It is convenient to monitor the choice of $\gamma^2\tilde{g}^{(2m)}$. The spread distribution of the occupancy numbers $\tilde{n}_\lambda$ of the shell-correction model has the important property that

$$\int_{-\infty}^{+\infty} F(E)\,\tilde{n}(E)\,dE = \int_{-\infty}^{\tilde{E}_F} F(E)\,dE,$$

if $E(F)$ is a smooth function of the energy in the sense indicated above. In particular, for $F(E) = E\tilde{g}(E)$ the latter equation means that for our definition of $\tilde{n}$ the model nucleus (the shell corrections are measured from the energy of this nucleus) remains in an unheated state notwithstanding the fact that the distribution $\tilde{n}$ is spread over a wide energy interval. Therefore there is no meaning to the interpretation, which seems legitimate at first glance, that (41) for $\delta\mathcal{U}$ is the excitation energy taken with the reverse sign of a nucleus heated to the temperature $\tilde{\gamma}$, from which the average value of the heating energy, which is equal to $\tilde{\gamma}^2\tilde{g}(E_F)$, is then

subtracted. Such an interpretation is actually possible for 2m = 0, but under these conditions meaningless results are obtained.

The quantity $\delta\mathcal{U}$ remains approximately the same for various shell-potential approximations also. Of course, here we are speaking of good models: The shell-correction model requires that the deviation of the average potential from the true one be minimal.

The shell corrections to the energy and the quantities associated with them are expressed in terms of three universal dimensionless functions $f(x)$, $n(x)$, and $f^*(x)$, which are respectively determined by Eqs. (32), (39), (45), and (46). These functions are shown in Fig. 4 for certain values of the degree 2m of the correcting polynomial.

4. THE GENERALIZED FORCES ASSOCIATED WITH SHELLS

As is evident from the preceding analysis, the first-order approximation in the shell-correction method turns out to be especially simple and consists in analyzing the variation of the total one-particle energy calculated for the average shell-model potential. This approximation does not depend explicitly either on the pairing interaction between nucleons or on the density variations $\delta\rho$. The second-order approximation contains these quantities explicitly [see Sec. 2, Eq. (17)]. However, it is easy to verify the fact that the first approximation for the shell correction is related to the shell variations of the particle density in a specific manner. Let us consider the derivative of $\delta\mathcal{U}$ with respect to a certain external parameter β on which it depends, since this parameter is included in the definition of the average field $\overline{V}$. For example, such a parameter may be the nuclear-surface deformation parameter or the radius R_0 of the nucleus. Taken with the opposite sign, this derivative is none other than the generalized force acting in the direction of the variable β, if the latter is treated as a certain generalized selective coordinate:

$$\delta F_\beta = -\partial\delta\mathcal{U}/\partial\beta. \tag{50}$$

Let $\Delta\overline{V}$ be the change in the average field due to a small change in β:

$$\Delta\overline{V} = \frac{\partial\overline{V}}{\partial\beta}\Delta\beta. \tag{51}$$

In the first order of perturbation theory the change in the one-particle energy is

$$\Delta E_\lambda = \int dv\Delta\overline{V}\,|\Phi_\lambda|^2. \tag{52}$$

Varying Eq. (31) for the level density, we find a change in the smoothed density:

$$\Delta\tilde{g}(E) = -\frac{1}{\gamma}\Sigma_\lambda(\Delta E_\lambda)\frac{\partial}{\partial E}f[(E_\lambda - E)/\tilde{\gamma}]. \tag{53}$$

Here we have replaced differentiation with respect to E_λ by differentiation with respect to E, which yields the same result except for the sign. Note that the condition requiring smallness of the perturbation in the expansion (52) is that the change in level energy must be small compared with the averaging interval $\tilde{\gamma}$. The change in level density may also be written as

$$\Delta g_\gamma(E) = -\int dv\,(\Delta\overline{V})\frac{\partial}{\partial E}\rho_\gamma(\mathbf{r}, E). \tag{54}$$

Here we have introduced the new quantity

$$\rho_\gamma(\mathbf{r}, E) = \frac{1}{\gamma}\Sigma_\lambda|\Phi_\lambda(\mathbf{r})|^2 f[(E_\lambda - E)/\gamma], \tag{55}$$

which may be interpreted as the nucleon density in phase space, averaged over the interval of γ near the energy E. The integral of $\rho_\lambda(\mathbf{r}, E)$ over the volume is equal to the level density

$$g_\gamma(E) = \int dv\rho_\gamma(\mathbf{r}, E), \tag{56}$$

while the spatial nucleon density averaged over the energy distribution is

$$\tilde{\rho}(\mathbf{r}) = 2\int_{-\infty}^{E_F} dE\rho_\gamma(\mathbf{r}, E) = 2\Sigma_\lambda|\Phi_\lambda(\mathbf{r})|^2\tilde{n}_\lambda. \tag{57}$$

Having made use of Eq. (41) for the shell correction, we find

$$\Delta(\delta\mathcal{U}) = \int dv\Delta\overline{V}\delta\rho^s(\mathbf{r}), \tag{58}$$

where

$$\delta\rho^s(\mathbf{r}) = 2\Sigma_\lambda|\overline{\Phi}_\lambda(\mathbf{r})|^2\delta n_\lambda. \tag{59}$$

Hence we obtain

$$\partial(\delta\mathcal{U})/\partial\beta = \int\frac{\partial\overline{V}}{\partial\beta}\delta\rho^s(\mathbf{r})\,dv. \tag{60}$$

This expression shows that the derivative of $\delta\mathcal{U}$ is related to the quantity $\delta\rho^s$, which represents the

oscillations of the spatial nucleon density which are caused by the nonuniform distribution of one-particle levels near the Fermi energy (i.e., by the energy shells).

Equation (60) may also be written in the form

$$\frac{\partial(\delta\mathcal{U})}{\partial\beta} = 2\Sigma_\lambda \langle\lambda|\partial\overline{V}/\partial\beta|\lambda\rangle\,\delta n_\lambda. \tag{61}$$

Noting that [21]

$$\langle\lambda|\frac{\partial\overline{V}}{\partial\beta}|\lambda\rangle = \partial E_\lambda/\partial\beta,$$

we find

$$\frac{\partial\delta\mathcal{U}}{\partial\beta} = 2\Sigma_\lambda\,(\partial E_\lambda/\partial\beta)\,\delta n_\lambda. \tag{62}$$

The derivative

$$-F_{p\lambda} = \partial E_\lambda/\partial\beta$$

characterizes the slope of the one-particle λ level in the diagram representing the one-particle spectrum as a function of the average-potential parameter β (for example, the slope of the level in the Nilsson diagram for a deformation equal to β ($F_{p\lambda}$ is the partial force of the level). Taking into account the form of the distribution δn (see Fig. 3), one can write

$$\delta F = F_{p>} - F_{p<},$$

where

$$F_{p\gtrless} = 2\Sigma_{E_\lambda\gtrless E_F} F_{p\lambda}\delta n_\lambda \tag{63}$$

is the resultant force of the levels situated above and below the Fermi energy, respectively, in an interval of order $\tilde{\gamma}$. Thus, the deforming shell force is a difference effect and is associated with the distribution nonuniformity near the Fermi energy.

In addition to δF_β it is also necessary to consider the classical forces corresponding to the liquid-drop portion of the complete expression for the binding energy of the nucleus (30), such as the surface-tension forces and the Coulomb forces. The total force is

$$F = F_{\text{Cou}} + F_{\text{sur}} + \delta F_\beta. \tag{64}$$

In particular, the shape-equilibrium condition is that the resultant of the forces acting on the surface shape must equal zero:

$$F_{\text{Cou}} + F_{\text{sur}} + \delta F_\beta = 0. \tag{65}$$

Since under ordinary conditions the drop terms considerably exceed the shell correction $\delta\mathcal{U}$, it follows that the shell force is also small compared with F_{Cou} and F_{sur}. The shell correction δF_β under the equilibrium condition (65) turns out to be substantial only near the equilibrium points of the drop model, where

$$F_{\text{Cou}} + F_{\text{sur}} \approx 0. \tag{66}$$

In the particular case of a small quadrupole deformation β_q we have

$$\partial\overline{V}/\partial\beta_q = \varkappa\hat{q}(\mathbf{r}), \tag{67}$$

where $\hat{q}(\mathbf{r})$ is the one-particle quadrupole-moment operator; $\varkappa$ is the coupling constant with the surface [22]. For the quadrupole shell force δF_q we obtain

$$\delta F_q = \varkappa\int d\nu\hat{q}\delta\rho^s = \varkappa\delta Q^s, \tag{68}$$

i.e., the shell force turns out to be proportional to the quadrupole moment of the distribution $\delta\rho^S$, which in turn is defined as the difference between the quadrupole moments $Q^S_>$ and $Q^S_<$ of the one-particle states situated above and below the Fermi energy. This additional force acts on the surface of the nucleus in the direction of the excess density (Fig. 5) in complete accord with the qualitative ideas of the combined Rainwater–Bohr–Mottelson model [22, 23], although $\delta\rho^S$ does not correspond either to the density distribution of an individual

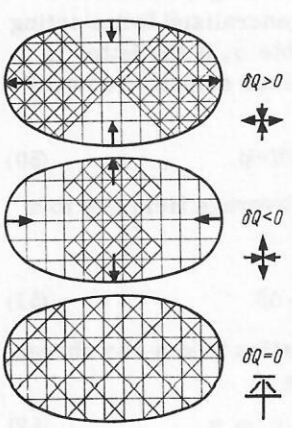

Fig. 5. The connection between the deforming shell force acting on the surface of the nucleus and the spatial variation of the nucleon density; the arrows indicate the direction of the forces. Equilibrium corresponds to $\delta Q = 0$.

particle (Rainwater) or to the nucleons of the unfilled shell (Bohr, Mottelson).

For the equilibrium shape corresponding to small deformation relative to a sphere, condition (66) is fulfilled and

$$\delta F = \varkappa \delta Q = 0,$$

i.e., the one-particle quadrupole moment of the nucleus coincides with its counterpart for the smoothed nucleon distribution $\tilde{\rho}^{s}(\mathbf{r})$. These problems will be considered in greater detail in connection with the problem of deformed nuclei in part II.

5. OSCILLATIONS OF THE NUCLEON DENSITY

The problem of the origin of oscillations of nucleon density in nuclei is of independent interest. This problem has been repeatedly investigated in the literature within the framework of the shell model [24]. Recent calculations of the nucleon distribution in nuclei, according to a perfected approximation of the Hartree–Fock type with phenomenological interaction that depends on local density, have shown that density oscillations also occur for an interaction which impedes the deviation of the density from the equilibrium value. The calculated slightly oscillating distribution is in agreement with data on high-energy electron scattering [25].

Above it was shown that a certain portion of the density oscillations is associated with the nonuniformity of the distribution of the one-particle states near the Fermi energy (with large shells), and it is precisely this component of the density oscillations that is associated with the shell variations of the binding energy of nuclei.

In the literature the existence of large shells is traditionally associated with the sphericity of the average one-particle potential or is explained by the similarity with the harmonic-oscillator potential. Such an interpretation has never been seriously substantiated; meanwhile, as specific calculations have shown, we are speaking of a very general phenomenon [12]. Appreciable nonuniformities of the shell type are revealed for practically any shape of the potential well and any one-particle potential. They remain, for example, when the spin–orbit parameters are increased severalfold in comparison with the normal value, although the magic numbers under these conditions are completely different. The presence of magic shells in deformed nuclei is of decisive significance in the problem of the origin of stable equilibrium deformations of nuclei and in the fission process [12, 26].

Formally the problem is to analyze the causes and conditions governing the appearance of substantial nonuniformities in the distribution of the eigenvalues of the homogeneous equation of the Schrödinger type. An analogous problem develops, for example, in the theory of radio-frequency and laser resonators when the necessity develops of concentrating the natural frequencies of the system in a restricted range. A rather extensive mathematical literature has been devoted to this problem: in particular, [27].

It has been shown that the existence of groups of eigenvalues corresponds to the appearance of simple periodic trajectories of classical motion which develop as envelopes of a group of eigenfunctions (see, for example, [27]). Here each of the eigenfunctions has little in common with the classical trajectory or with the other functions of the group. Regrettably, it is only quite recently that the possibility was noted of such an interpretation of shell phenomena in nuclei. Balian and Bloch [28] consider the Green's function for the one-particle problem, which has been averaged over a finite energy interval γ. The level density averaged over the interval is

$$g_{\gamma}(E) = \frac{1}{\pi}\int dE' \frac{\gamma}{(E-E')^2+\gamma^2}\Sigma_{\lambda}\delta(E'-E_{\lambda}) = \frac{1}{\pi}\operatorname{Im}\operatorname{Tr}[(E-H-i\gamma)^{-1}]. \quad (69)$$

This quantity is expressed in terms of the averaged Green's function, in terms of which one may also express the distribution of the nucleon density in space, averaged over energy. Such a Green's function is determined by the Schrödinger equation with the complex energy $\tilde{E} = E + i\gamma$. For a sufficiently large averaging interval γ and quasiclassical motion far from the reversal points the solution corresponds to the Thomas–Fermi approximation with a characteristic smooth distribution. For a smaller but finite γ, oscillations develop in the energy and spatial distributions of the nucleons, which are associated with the stationary classical periodic trajectories. Several such trajectories are shown in Fig. 6 in a spherical potential well with infinitely high walls. Trajectories of each type are characterized by a periodic dependence on the magnitude of the wave vector $\mathbf{k}$ with a period of the order of

$$\Delta k \approx \pi/2R, \quad (70)$$

where 2R is a quantity of the order of the size of

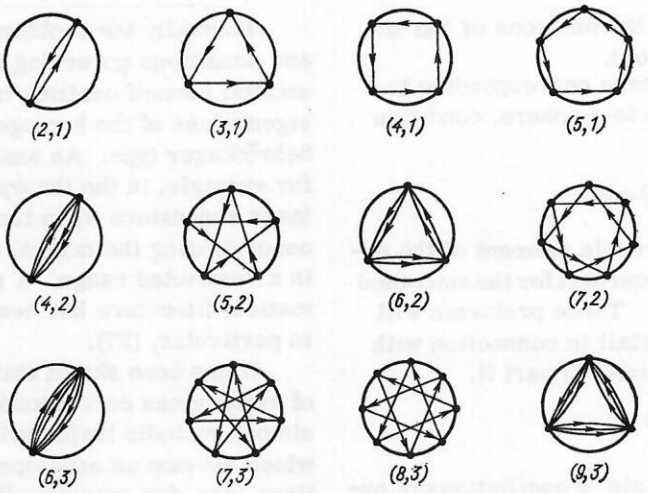

Fig. 6. Periodic trajectories of a particle in a spherical potential well, with which large nucleon shells are associated. Each such trajectory corresponds to a group of quantum one-particle states and a bunch of one-particle energies. The numbers in parentheses are the classifications of the periodic orbits in accordance with Bloch and Balian [28]; the first number is the number of vertices, and the second is the number of rotations about the center.

the system. This corresponds to an energy period of the order of

$$\Delta E \approx E_F (\pi/k_F R) \approx \frac{1}{2} E_F A^{-1/3}, \qquad (71)$$

where k_F is the momentum for the Fermi energy E_F. This estimate is in agreement with the quantity $\hbar\Omega$. During averaging the simpler trajectories have a larger value [28]. The periodic trajectories are characterized by a different degree of stability relative to variations of the shape of the well, and it may be assumed that precisely this factor leads to stabilization of shells of one type of shape of a given nucleus and to a reduction of the stability of other shapes.

Unfortunately, the formal method developed in [28] is poorly suited to specific calculations, especially when realistic potentials are used and when the shape of the nucleus is arbitrary. In practice it is simpler to obtain the solution of the one-particle problem by means of one of the existing numerical methods [19], and then to isolate the oscillating components as described above. Such an approach has great generality and is more flexible. The connection between our method and the Balian–Bloch papers, which have great significance for a qualitative understanding of the results of calculations performed according to the shell-correction model, is quite obvious.

Let us also note the paper by A. S. Tyapin [29], in which it was shown that the shell oscillations of the one-particle energy may be determined analytically as the correction terms for the correct substitution of integrals for the sums over the levels. Here the same results were obtained as those obtained for a numerical averaging in the shell-correction model. The applicability of the Tyapin model is limited by the fact that it is necessary to know the analytic expression for the one-particle spectrum.

Shell oscillations are a consequence of the closed nature of the potential-well volume (i.e., in the final analysis they are a consequence of the finiteness of the nuclear size). In a system of noninteracting particles oscillations of the spatial density of the nucleons, which are not related to the shells, are also possible. Kohn and Sham [30] focused attention on the fact that density oscillations also develop for a system of independent particles in a space bounded by a reflecting plane wall. The amplitude of such oscillations decreases with departure from the edge, and thus we are speaking of a certain surface phenomenon. The origin of this effect is easy to understand. Near the wall all wave functions vanish, and the total density is expressed in the form

$$\rho(z) = \text{const} \int\limits_{(k^2 < k_F^2)} d\mathbf{k} \sin^2(k_z z), \qquad (72)$$

where z is the coordinate in the direction perpendicular to the wall. From this expression we find

$$\rho(z) = \rho(\infty)\left(1 + 3\frac{\cos x}{x^2} - 3\frac{\sin x}{x^3}\right), \qquad (73)$$

where $r = 2k_F Z$. The density (72) oscillates near the edge with a period

$$\Delta z \approx \pi/k_F, \qquad (74)$$

the amplitude of the oscillations decreasing as $1/z^2$ (Fig. 7). The first two terms in (73) coincide with the Kohn–Sham asymptotic equation.

It is clear that such a trivial effect must also be present in the shell model, especially in those cases when the average potential has a sufficiently sharp boundary (as, for example, in the Woods–Saxon model). It may be isolated by using the fact that, unlike shell oscillations, edge oscillations depend weakly on the Fermi energy. Consequently, they must be present in oscillations of the nucleon density after averaging over a spectrum with $\gamma \approx \tilde{\gamma}$, whereas shell oscillations must vanish. Let us consider the results of specific calculations from these standpoints. Above we have already introduced four different functions characterizing the spatial distribution of the nucleons, namely: the nucleon density $\overline{\rho}^c$ in the self-consistent problem, the statistically averaged distribution $\overline{V}$ with which the average shell-model potential ρ^s is associated, the density $\overline{V}$ for the nonself-consistent problem, in which ρ^s is the external potential (the density in the shell model), and, finally, ρ^s, which was obtained with a distribution of the occupancy numbers $\tilde{n}_\lambda$ that was "spread" over the shells. As is evident from (60), for shell variations of the binding energies of nuclei the quantity

$$\delta\rho^s = \rho^s - \tilde{\rho}^s \qquad (75)$$

is important, and in the spirit of the qualitative

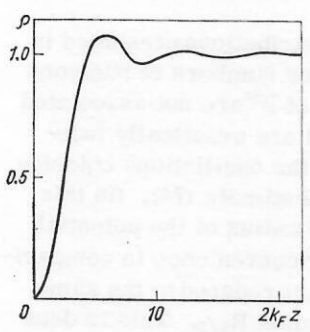

Fig. 7. Density oscillations near an infinite wall (the Kohn–Sham effect) [30].

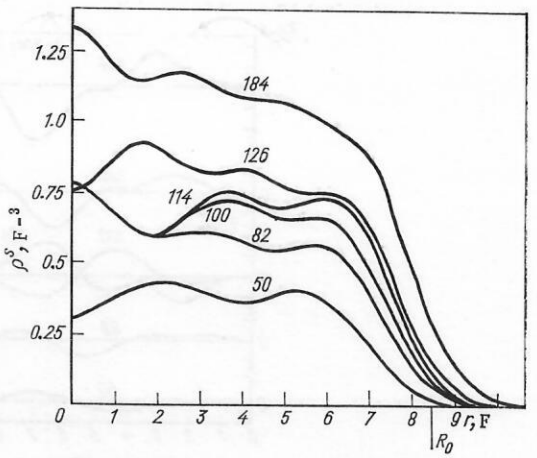

Fig. 8. Shell density of the neutrons $\rho^s(r)$ in the Woods–Saxon model. The potential well is for the Z = 114, N = 184 nucleus. The curves are given for various occupancies of the levels of the well, which correspond to the indicated numbers of nucleons.

considerations expounded above it is natural to associate precisely this quantity with the shell oscillations of the density due to classical periodic orbits.

Several examples of the density distributions ρ^s and $\tilde{\rho}^s$ have been given in Figs. 8 and 9. The conventional spherical potential of the Woods–Saxon model was used in the calculations. In order to avoid the complications associated with a shallow

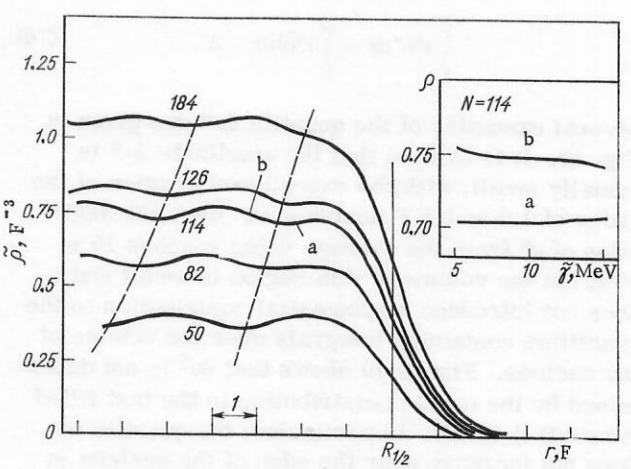

Fig. 9. Density of the neutrons in the shell model that has been smoothed over the energy distribution for the same numbers of the filled levels and the same potential well as those shown in Fig. 8. The oscillations of $\tilde{\rho}^s$ do not depend on the occupancy of the shells and qualitatively correspond to the Kohn–Sham effect. The uniqueness with which the oscillations of $\tilde{\rho}^s$ are determined is illustrated in the insert, where the values of $\tilde{\rho}^s$ (r) are shown on a magnified scale at two points, corresponding to the maximum (b) and minimum (a). For convenience in comparing the curves the half-density radii $R_{1/2}$ are made to coincide.

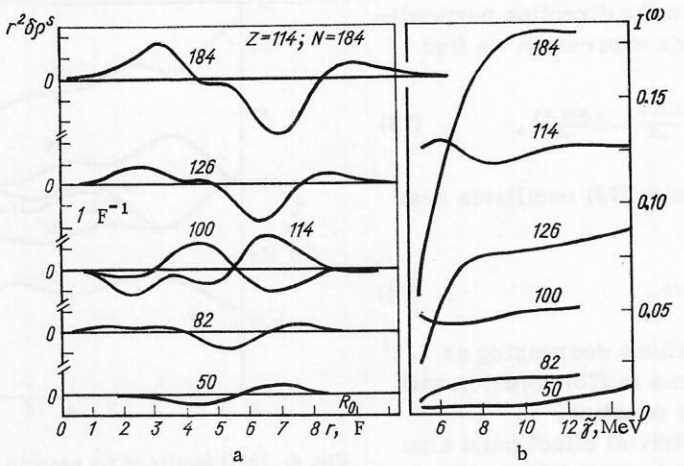

Fig. 10. The shell component of the oscillations $\delta\rho^s(r)$ of the one-particle density (a) for different numbers of filled levels of the well, and the integral (77) of the square of $\delta\rho^s$, which determines the scale of the second approximation of the shell-correction model (b). The independence of I^0 from $\tilde{\gamma}$ shows the uniqueness of the determination of $\delta\rho^s$.

depth of the Fermi energy in the potential well, a potential was used corresponding to a nucleus with Z = 114 and N = 184. Because of the large radius of the well, more bound states will occur in it; this allows a comparatively wide interval $\tilde{\gamma}$ to be used. The radial functions are normalized to unity in integration over the radius, so that

$$\int_0^\infty r^2\rho^s\,dr = \int_0^\infty r^2\tilde{\rho}^s\,dr = N. \qquad (76)$$

Several examples of the quantity $\delta\rho^S$ are given in Fig. 10. It is evident that the amplitude $\delta\rho^S$ is actually small, with the exception of a region of the order of 1.0 to 1.5 F near r = 0. Here the deviation of ρ^S from the average value reaches 15 to 20%, but the volume of this region is small and it does not introduce a substantial contribution to the quantities containing integrals over the volume of the nucleus. Figure 10 shows that $\delta\rho^S$ is not determined by the nucleon distribution in the last filled subshell (j level). In particular, the quantity $\delta\rho$ does not increase near the edge of the nucleus in those cases when a subshell with a large angular momentum is filled. Near the edge of the nucleus the amplitude of $\delta\rho^S$ is small, and this region also does not make a special contribution to the shell corrections.

The distribution of $\delta\rho^S$ varies only slightly as the radius of the potential well increases, notwithstanding the considerable increase in the number of levels which are taken into account in calculating the average value. Actually, only the amplitude of $\delta\rho^S$ varies, decreasing in proportion to the cube of the well radius.

A characteristic feature of the Woods–Saxon model is the fact that the amplitude of the density oscillations which are associated with the shell ($\delta\rho^S$) is considerably smaller than the variation of the quantity ρ^S. In accordance with Eq. (75) this means that the energy-smoothed distribution $\tilde{\rho}^S$ retains a considerable fraction of the oscillations in this case. The oscillations remaining are naturally interpreted as being due to the Kohn–Sham edge effect. However, first of all one should be convinced that the oscillations are isolated uniquely when spread occupancy numbers $\tilde{n}_\lambda$ are used which are obtained from the average quantities in Sec. 3 (see Fig. 9). Figure 9 shows (on a magnified scale) the values of one of the functions $\tilde{\rho}^S$ taken at the minimum and maximum. The uncertainty associated with the choice of the parameter $\tilde{\gamma}$ does not exceed several percent of the amplitude of the oscillations of $\tilde{\rho}^S$.

A comparison of the distributions presented in Fig. 9 calculated for various numbers of nucleons shows that the oscillations of $\tilde{\rho}^S$ are not associated with the shell structure and are practically independent of N, the period of the oscillations coinciding approximately with the estimate (74). (In this case $k_F \sim N^{-1/3}$, since the radius of the potential well does not change.) For convenience in comparison, all of the distributions are reduced to the same value of the half-density radius $R_{1/2}$. This is done

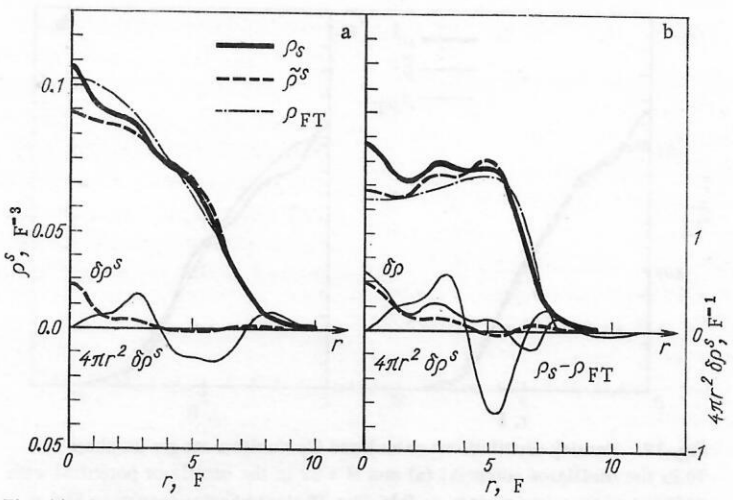

Fig. 11. Various proton-density distributions and the shell correction to the spatial density, which have been calculated for the Pb^{208} nucleus by means of the Nilsson model (a) and the Woods–Saxon model (b): The Thomas–Fermi distributions ρ_{TF} were calculated without the l^2 term as well. In calculations with the Woods–Saxon model the Coulomb potential was taken into account [13].

because, although all of the distributions are calculated in the same well, the lengths of the distribution tails in the classically forbidden region differ as a function of the position of the Fermi level in the well, as a consequence of which the effective radius of the density turns out to be somewhat larger for a greater number of nucleons. This evidently also explains the smaller amplitude of the edge maximum for the greatest number of nucleons N = 184 when the difference from the infinitely high wall approximation is felt more strongly.

The amplitude of the residual oscillations of $\tilde{\rho}^s$ must decrease in the Nilsson model or in a purely harmonic oscillator, where the nucleon distributions for deep states are characterized by a varying radius and averaging takes place also over the distribution radius during integration over the states in Eq. (72) (this leads to additional smoothing of the oscillations). This qualitative reasoning is in agreement with the numerical calculations. Contrary to the Woods–Saxon model, the amplitude of the residual oscillations of ρ^s in the Nilsson model is small, while for a simple harmonic oscillator $\tilde{\rho}^s$ is practically no different from the smoothed quasiclassical distribution of the Thomas–Fermi model, of course with the exception of the classically forbidden region, where the Thomas–Fermi density is zero, while $\tilde{\rho}^s$ is finite but exponentially small (Figs. 11 and 12; see also [31]).

Unlike $\tilde{\rho}^s$ the density oscillations $\delta\rho^s$ are associated only with the energy shells in the one-particle level distribution near the Fermi energy. For these, close results are obtained in various realistic models (see, for example, Figs. 8, 10, and 11, where the calculations are shown for Z = 82 in the Woods–Saxon model and the Nilsson model). These different models reflect close distributions of the one-particle levels near the Fermi energy. Several examples of $\delta\rho^s$ for various N have been shown in Fig. 10. For convenience in representing $\delta\rho^s$, which is very small for intermediate values of the radius, this quantity has been multiplied by r^2. At the right the integral

$$I_0 = \int_0^\infty r^2\,(\delta\rho^s)^2\,dr \qquad (77)$$

is shown as a function of the parameter $\tilde{\gamma}$. The approximate constancy of this quantity as a function of $\tilde{\gamma}$ is evidence of the uniqueness of the determination of $\delta\rho^s$. The integral (77) may serve to estimate the scale of the terms of order $(\delta\rho)^2$ in Eqs. (15) and (17). In order to estimate the magnitude of the shell correction and the terms of higher order formally, it is necessary to know the amplitude of $\delta\rho$ in the nuclear volume. Let us assume that the difference between ρ^s and $\tilde{\rho}^s$ is determined by the density fluctuation in the last shell. Since a large shell contains an average of $A^{2/3}$ nucleons, the mean-square fluctuation of the number of particles associated with the shell is equal to

$$\Delta A \approx \int_0^\infty r^2 \sqrt{(\delta\rho^s)^2}\,dr \approx A^{1/3},$$

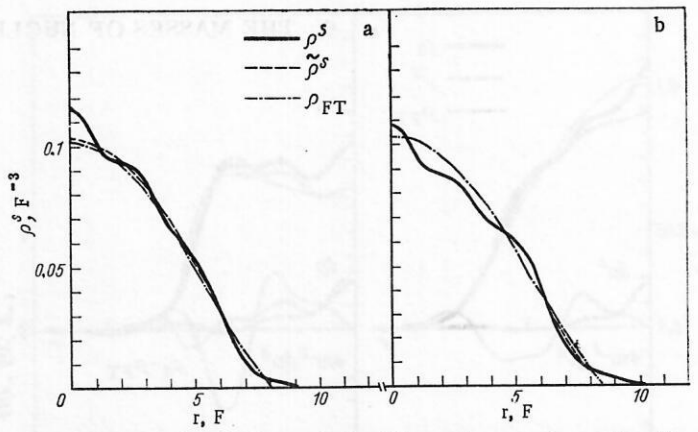

Fig. 12. Density distributions calculated for nucleon magic numbers N = 70 in the oscillator potential (a) and N = 82 in the oscillator potential with addition of the spin–orbit term (b): The Thomas–Fermi density in Fig. 6 practically coincides with the density smoothed over the shells, with the exception of the classically forbidden region at r > 7 F.

i.e., of the order $A^{-2/3}$ relative to the total number of particles. In numerical calculations a value of the order of several units is obtained for the quantity ΔA. Thus, the average value is

$$\delta\rho/\rho \sim A^{-2/3}. \tag{78}$$

Now let us estimate the amplitude of the shell variation $\delta\mathcal{U}$ of the binding energy of the nucleus. For this purpose let us make use of Eq. (60), where $\Delta\overline{V}$ corresponds to the change in the average potential $\overline{V}$ caused by a difference in the number of nucleons by an amount of the order of $A^{2/3}/2$, which corresponds to a transition from a magic nucleus to the middle of the shell. The variation of $\overline{V}$ can be reduced to the variation of the volume v of the potential well by an amount of the order of $\Delta v/v \approx A^{-1/3}/2$. For the variation of the shell correction from the magic nucleus to the middle of the shell we have the estimate

$$\Delta(\delta\mathcal{U}) \approx E_F \delta\rho \Delta v \approx \frac{1}{2} E_F \approx 20 \text{ MeV} \tag{79}$$

(the depth of the central well is assumed to equal $E_F \approx 40$ MeV). For the maximum amplitude of the variation of the shell correction this estimate agrees with the values found in numerical calculations for spherical nuclei. Actually, however, the variation of the shell correction in the transition to the middle of a large shell turns out to be smaller than the estimate (79) as a result of the fact that the shape of the nucleus changes.

The estimate of the magnitude of the second-order terms in (15) is determined by taking the first iteration in Eq. (23) for Γ and replacing the pairing interaction by a δ function there:

$$v(1, 2) \approx f_0 (dE_F/d\rho)\, \delta(\mathbf{r}_1 - \mathbf{r}_2),$$

where the coefficient $f_0 \approx 1$ [17]. In this case we have

$$I \approx \frac{1}{9} f_0 E_F r_0^3 I_0.$$

Numerical calculations yield values less than 1 to 2 MeV for I. Values close in magnitude are obtained in more exact calculations with an amplitude Γ calculated according to the theory of finite Fermi systems [14]. Using (78), we find the formal estimate

$$I \approx \frac{f_0}{3} E_F \frac{1}{A^{1/3}} \approx \frac{1}{A^{1/3}} \delta\mathcal{U}.$$

The residual oscillations $\tilde{\rho}^s$ are a consequence of the extreme assumption of total independence of the motion of all of the particles in the nucleus and evidently must be absent in real cases as the result of the increasing influence of nucleon correlations for the deeper states. However, this has no significance for calculations of shell phenomena, since it has been shown that even such an oscillating distribution is a smooth function of the atomic number, the deformation,[2] etc. This allows it to be identified with the statistically averaged distribution $\tilde{\rho}^s$, which is introduced in substantiating the

[2] V. V. Pashkevich showed that the smoothness is preserved for an arbitrary deformation of the nucleus.

shell-correction model. The appearance in the shell-correction method of several densities which characterize the spatial distribution of the nucleons creates the possibility of a new approach to the problem of determining the collective variables of the nuclear shape. Actually, it is quite natural to determine the collective shape variables from the smoothed distribution $\bar{\rho}$ for example, from the magnitude of the quadrupole moment of this distribution:

$$\tilde{Q} = \int \hat{q}\bar{\rho}\, dr. \qquad (80)$$

Such a shape distribution is a very convenient generalization of the method adopted in the statistical model of nuclei [32], where the shape of the nucleus is determined from the smoothed Thomas–Fermi density distribution. Thus, one may reject the requirement of microscopic self-consistency for the collective variables, which introduces great difficulties and actually does not allow changes in shape to be distinguished from small density oscillations in the volume of the nucleus.

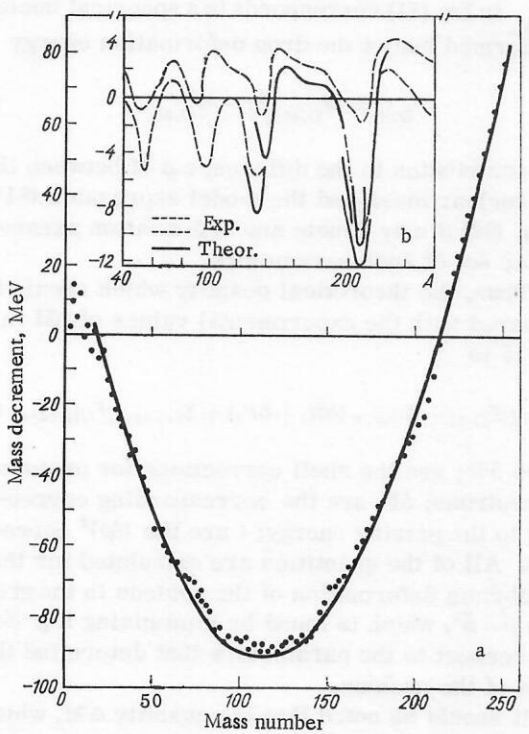

Fig. 13. Shell effect in nuclear masses: a) dependence of the mass decrement of the nuclei on the mass number [34]; b) calculated shell corrections for the ground states of spherical and deformed nuclei are compared with the deviations of the experimental masses from the drop value for the spherical nucleus; the experimental values correspond to the region between the two dashed curves [12].

6. THE MASSES OF NUCLEI

Calculation of the masses of nuclei is one of the principal applications of the shell-correction method. In this part of the paper we shall consider only certain problems associated with calculations of shell corrections to the drop masses of spherical nuclei.

The general pattern of the shell variations of nuclear masses is depicted in Fig. 13. A fairly close agreement between the theoretical calculations and the experimental results can be seen. It should be noted that in these calculations one of the simple initial versions of the Nilsson model was used, and no parameters were introduced. Subsequently, similar calculations, but in a somewhat different context, were carried out by Seeger [33], and the total nuclear mass had the following form:

$$M(N, Z) = M_{\text{D.M.}}(N, Z) + \Delta M(N, Z),$$

where ΔM (N, Z) is the calculated shell correction. This expression is used for the simultaneous fitting of the parameters of the drop model (D. M.) and of the Nilsson potential on the basis of best agreement with the experimental masses.

It is of interest that Nilsson-potential parameters which are very close to the conventional ones obtained by fitting the one-particle spectrum are obtained in this manner. Although such calculations are still far from perfect, fairly good agreement was found for almost 1000 nuclei with a mean-square deviation of 0.6 to 0.7 MeV, i.e., the deviation is approximately the same as it is for the phenomenological approach when many additional special parameters are introduced in order to describe the shell corrections to the masses. This error should be compared with the 2-3 MeV magnitude of the mean-square deviation from the experimental masses for the simple drop model. Nilsson, Thompson, and Tsang [35] recently performed calculations of the shell corrections to nuclear masses using the latest version of the Nilsson model. Although under these conditions no significant improvement of the mean-square deviation was achieved, it was shown that in the calculations even the comparatively fine structure of the empirical shell corrections (Fig. 14) is reproduced.

Unfortunately, because of technical difficulties no systematic calculations of this kind have yet been carried out with the more realistic potential of the Woods–Saxon model. Available results for several individual cases are in agreement with the results of the Nilsson model. In calculations of

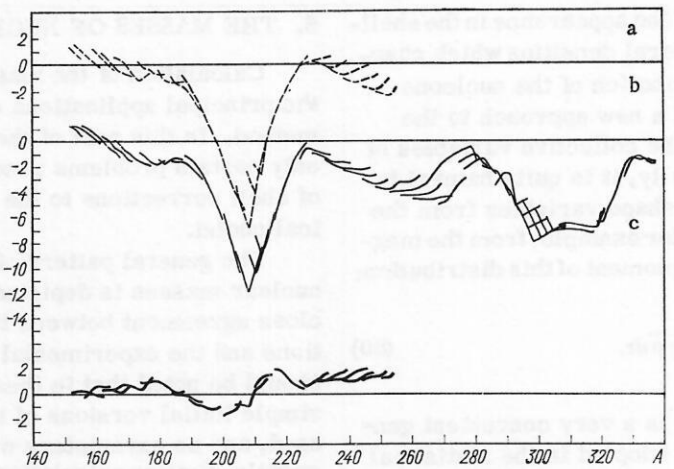

Fig. 14. Shell corrections to the Weizsäcker equation (of the drop model): a) experimental values (MeV); b) calculation with the improved Nilsson model (MeV); c) discrepancy between the theoretical and experimental values (MeV) in accordance with [35]. The calculations took into account pairing of nucleons in the Bardeen–Cooper–Schrieffer approximation.

nuclear masses it is necessary to consider the residual interactions more precisely; these were considered only in the form of Cooper pairing in all of the papers [13, 18, 33, 35]; one should also consider the term $(\delta\rho)^2$, which was not considered in the principal approximation of the shell-correction model and also depends on the residual interaction.

Deviations of experimental nuclear masses from the "smooth" drop-model approximation can be found in many papers devoted to the phenomenological description of nuclear masses. These deviations depend comparatively weakly on the specific form of the expression used for the smooth part, and they may be treated as completely definite empirical data (Fig. 15), where the Myers–Swiatecki data are presented [7]. The figure shows the difference between the experimental nuclear mass and the calculated drop value as a function of the number of neutrons N and the number of protons Z. As usual, the drop value also includes a correction for the even–odd effect (the so-called pairing energy), i.e.,

$$M_{\text{D.M.}} = M^0_{\text{D.M.}} + (11{,}0/A^{1/2})\,\delta,\ \text{MeV}, \qquad (81)$$

where

$$\delta = \begin{cases} +1 \text{ for an even nucleus,} \\ 0 \text{ for an odd nucleus,} \\ -1 \text{ for an odd–odd nucleus.} \end{cases}$$

The correction (81) eliminates even–odd fluctuations of the empirical masses. Note also that $M^0_{\text{D.M.}}$ in Eq. (81) corresponds to a spherical nucleus. In deformed nuclei the drop deformation energy

$$\mathscr{D}_{\text{D.M.}} = M_{\text{D.M.}}(\beta) - M^0_{\text{D.M.}} \qquad (82)$$

also contributes to the difference ΔM between the real nuclear mass and the model expression (81). In Eq. (82) β may denote any deformation parameter or set of such parameters.

Thus, the theoretical quantity which should be compared with the experimental values of ΔM in Fig. 15 is

$$\Delta M = [\mathscr{D}_{\text{D.M.}} + \Sigma_{i=p,\,n}(\delta\mathscr{U}_i + \delta P_i) + \Sigma_{i,\,j=p,\,n} I_{ij}]_{\beta=\beta^*}, \qquad (83)$$

where $\delta\mathscr{U}_i$ are the shell corrections for protons and neutrons; δP_i are the corresponding corrections to the pairing energy; I are the $(\delta\rho)^2$ corrections. All of the quantities are calculated for the equilibrium deformation of the nucleus in the ground state $\beta = \beta^*$, which is found by minimizing Eq. (83) with respect to the parameters that determine the shape of the nucleus.

It should be noted that the quantity ΔM, which is found from Eq. (83), is compared directly with the experimental values of the mass defects of the individual nuclei, whereas it is usually the practice in microscopic theory to consider more or less complex combinations of the masses of individual

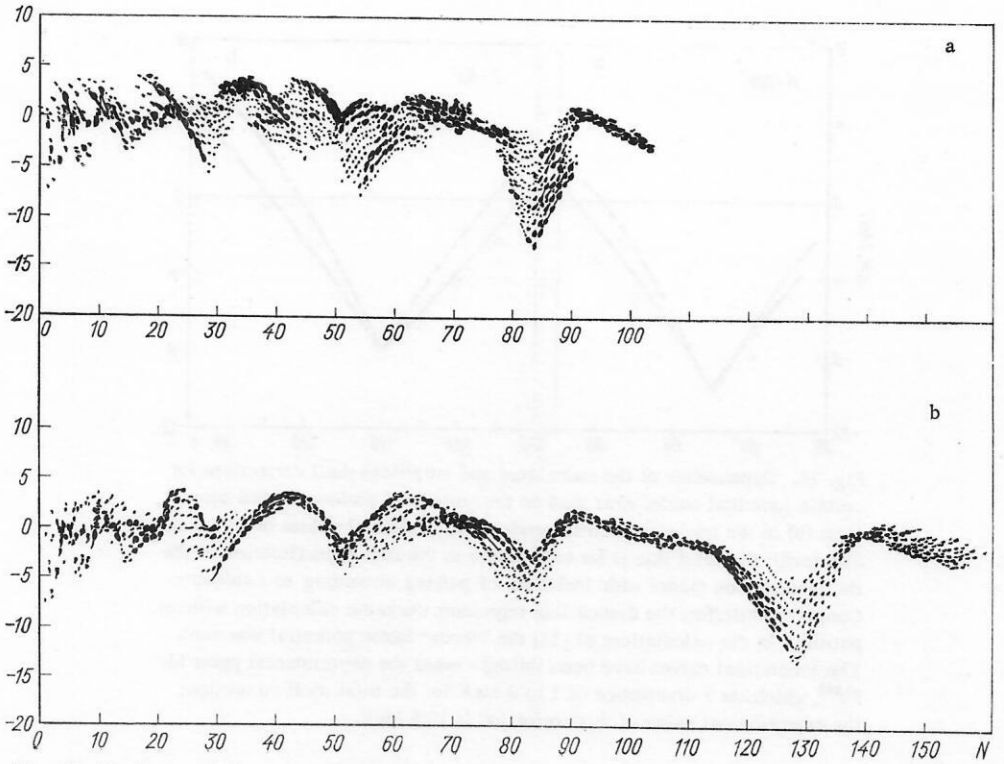

Fig. 15. Deviation of the experimental masses of the nuclei (MeV) from the drop-model value for a nucleus having a spherical shape, as a function of the number of protons (a) or neutrons (b) in the nucleus [7].

nuclei in order to avoid the contribution from terms of the drop-model type (as, for example, in the approach based on the Fermi-liquid theory [17]). In order to illustrate the possibilities of the method and the specific problems that develop we shall consider the range of spherical nuclei near the doubly magic nucleus ^{208}Pb in greater detail below.

First of all, let us note an important feature of the empirical values of ΔM presented in Fig. 15. It is evident that in spherical near-magic nuclei all ΔM_n determined as a function of the number of neutrons for a given number of protons are represented in the form of a series of approximately parallel curves. The magnitude of the shift for a change in Z is equal to the increment ΔM considered as the function of Z for a given N. A similar pattern occurs also for the dependence on N. This means that in the first approximation the empirical shell corrections may be represented in the form of a sum of partial shell corrections for neutrons and protons separately, which are independent of each other:

$$\Delta M(N, Z) \approx \Delta M_n + \Delta M_p \qquad (84)$$

in accordance with the principal terms of Eq. (83). Thus, knowing ΔM_n for several values of the number of protons (ΔZ), and ΔM_p for several values of the number of neutrons (ΔN), we obtain the shell corrections ΔM for $\Delta N \Delta Z$ of the individual nuclei. From the data presented in Fig. 15 it is evident that this holds for approximately 20 to 30 even nuclei near lead, and the inaccuracy of the approximation (84) does not exceed 0.5 MeV in this region. For a large departure from a magic nucleus the parallelness of ΔM_n and ΔM_p is destroyed, which may be caused by a change in the shape of the nucleus. On the basis of the data indicated one can already draw the conclusion that the magnitude of the interaction terms I_{ij} in Eq. (83) is small. Actually, the amplitude of the effective proton–neutron pairing interaction between a particle and a hole in nuclei of the same order even exceeds the amplitude of nn or pp interactions, while the np interaction term I_{np} in Eq. (83) turns out to be so small that it does not have a substantial effect on the independence of the partial ΔM_n and ΔM_p. Such an approach is substantiated by the results of numerical calculations of the second-order correction in $\delta\rho$, for which values not exceeding 1 MeV are obtained in the region of lead [14].

This property allows a certain simplification of the comparison between the theoretical and experimental values. First let us determine the best

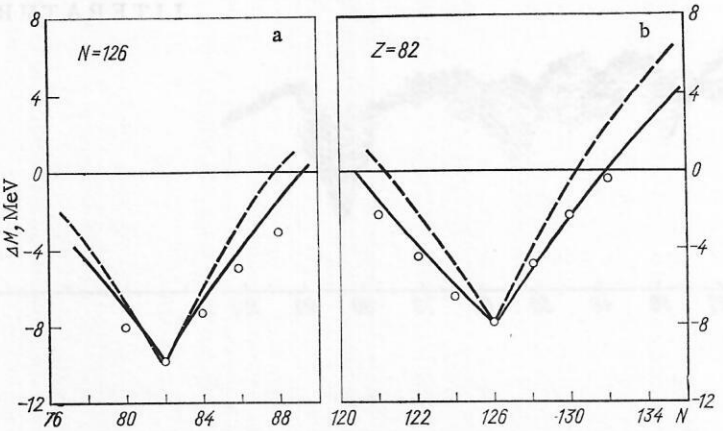

Fig. 16. Dependence of the calculated and empirical shell corrections for certain spherical nuclei near lead on the number of protons (a) and neutrons (b) in the nucleus: O corresponds to the empirical values of Myers and Swiatecki; the solid line is for calculation in the first approximation of the shell-correction model with inclusion of pairing according to Bardeen–Cooper–Schrieffer; the dashed line represents the same calculation without pairing. In the calculations of [13] the Woods–Saxon potential was used. The theoretical curves have been shifted toward the experimental point for Pb^{208}, which has a divergence of 1 to 3 MeV for the total shell correction; the experimental value of this correction is 13.5 MeV.

experimental partial shell corrections for neutrons and protons. For example, the neutron corrections may be obtained by averaging the quantity $\Delta M(Z, N+2) - \Delta M(Z, N)$ over several values of Z for each number of neutrons N. The same may also be done for the proton correction [13]. The average partial corrections may be used as experimental values in the approximation based on Eqs. (84) (Fig. 16). Note that from data in Fig. 15 one cannot determine the absolute values of ΔM_n and ΔM_p separately, since only their sum ΔM is found from the experiments (it is equal to 12.8 MeV for ^{208}Pb). Thus, the matter can be reduced to separate consideration of the relative changes ΔM_n and ΔM_p as functions of N and Z, and to the problem of the correspondence between the sum of these quantities and the total shell correction for one of the nuclei (for example, ^{208}Pb).

An interesting feature of the distribution of the empirical values of ΔM near magic nuclei is that the slope of the straight lines ΔM_n and ΔM_p differs considerably on opposite sides of the magic number of nucleons. Thus, from Fig. 15 it follows that the value of ΔM increases on an average by 2.3 MeV for a growth of N by two units, whereas to the left of N = 126 the value of ΔM increases only by 1.1 MeV for a reduction of N by two units. For protons near Z = 82 the corresponding increments are 2.3 and 1.2 MeV. A similar pattern is also observed near other magic numbers. From Fig. 16 it is evident that this feature can be reproduced well in calculations, in contrast to the usual phenomenological equations [7].

It is of interest to clarify what this difference is due to. For this purpose we consider the variation of the shell correction for a variation of the number of nucleons by two units. Directly from the definition of $\delta\mathcal{U}$ we have

$$\delta\mathcal{U}(N+2) - \delta\mathcal{U}(N) \approx 2[E_{N+2} - \tilde{E}_F(N)]; \quad (85)$$

$$\delta\mathcal{U}(N-2) - \delta\mathcal{U}(N) \approx 2[\tilde{E}_F(N) - E_N], \quad (86)$$

where $\tilde{E}_F$ is the Fermi energy for the "smooth" distribution; E_{N+2} and E_N are the energies of the last filled one-particle levels for N + 2 and N. The sum of the quantities (85) and (86) for N = 126 corresponds to the difference between the increments to the right and to the left of the magic number N = 126. This quantity is equal to

$$4\{1/2(E_{N+2} + E_N) - \tilde{E}_F\}. \quad (87)$$

It is evident that the difference between the slopes is associated with the deviation of the position of $\tilde{E}_F(N)$ from the average value inside the gap between the two closest levels of large shells. As a result of the fact that the number of nucleons in the higher (larger) shells is greater, the Fermi

energy for the smoothed distribution turns out to be below the middle of the gap, which leads to a special asymmetry of the particles and holes (see the dashed curves in Fig. 16).

The asymmetry effect practically vanishes if the pairing of nucleons is taken into account in the Bardeen–Cooper–Schrieffer approximation (see solid curves in Fig. 16). This takes place because the pairing energy turns out to be considerably higher in the case of a pair of particles that has been added to the magic core in a state having a higher angular momentum than that corresponding to a pair of holes in the state with a small angular momentum $p_{3/2}$ [13]. The Bardeen–Cooper–Schrieffer theory is inaccurate for a small number of particles outside the magic core, but it is evident that even in this simple approximation the agreement with experiment is not bad.

An even better agreement is obtained for ΔM_{np} in individual nuclei near lead if the distance between all levels of the two neighboring shells of ^{208}Pb is reduced by approximately 1.6 MeV. Formally this is equivalent to adding a constant pairing energy of 1.5 MeV for each pair of particles or holes relative to a doubly magic core. The discrepancy between the calculated values of ΔM_{np} and the experimental values in individual nuclei then does not exceed 0.2 MeV. This result compels us to assume that it is precisely such a simple effect to which the influence of the pairing interaction reduces.

The discrepancy of several MeV in the magnitude of the shell correction ^{208}Pb is in full agreement with the accuracy of the principal approximation of the shell correction. The comparison between the results of the calculations and other versions of the one-particle model showed that the difference also is within the limits of the theoretical estimate of the error (of the order of $A^{-1/3} \approx 20\%$).

It is quite possible that the accuracy of calculations of the masses of spherical nuclei can be considerably increased after terms of order $(\delta\rho)^2$ have been taken into account and a better approximation of the theory of pairing correlations has been used. However, in many other cases, especially in the theory of deformed nuclei, sufficient accuracy is provided by the simple first approximation of the shell-correction model and the Bardeen–Cooper–Schrieffer approximation for pairing correlations. Applications of the shell-correction model to the theory of deformed nuclei and fission will be described in the second part of the review.

LITERATURE CITED

1. A. De-Shalit and I. Talmi, Nuclear Shell Theory, Academic Press, New York (1963).
2. A. Bohr, Proc. Int. Conf. on Nuclear Structure, Tokyo (1967).
3. B. Mottelson and S. G. Nilsson, Phys. Rev., 99, 1615 (1955).
4. D. R. Bes and Z. Szymanski, Nucl. Phys., 28, 42 (1963).
5. S. T. Belyaev, Mat.-Fys. Medd. Danske Vid. Selskab., 31, 11 (1959).
6. W. D. Myers and V. J. Swiatecki, Nucl. Phys., 81, 1 (1966).
7. W. D. Myers and V. J. Swiatecki, Proc. Int. Symp., "Why and How...," Lysekil, Sweden (1966), Almquist and Wiksell, Stockholm (1968), p. 343.
8. V. M. Strutinsky, Phys. Chem. Fiss., 1, 171 (1965).
9. B. T. Geilikman and G. I. Khlebnikov, Yad. Fiz., 7, 215 (1968).
10. V. M. Strutinskii, Yad. Fiz., 3, 613 (1966).
11. V. M. Strutinsky, Nucl. Phys., A95, 420 (1967).
12. V. M. Strutinsky, Nucl. Phys., A122, 1 (1968).
13. M. Brack, J. Damgaard, et al., Rev. Mod. Phys., 44, 320 (1972).
14. G. G. Bunatian, V. M. Kolomietz, and V. M. Strutinsky, Nucl. Phys., A188, 225 (1972).
15. H. A. Bethe, Preprint, Cornell Univ., Ithaca, 14850 (1971).
16. H. A. Bethe, Phys. Rev., 167, 879 (1968).
17. A. B. Migdal, Theory of Finite Fermi Systems and the Properties of Atomic Nuclei [in Russian], Nauka, Moscow (1965).
18. S. G. Nilsson et al., Nucl. Phys., A131, 1 (1969).
19. J. Damgaard et al., Nucl. Phys., A135, 432 (1969).
20. W. Lin, Phys. Rev., C2, 871 (1970).
21. L. D. Landau and E. M. Lifshits, Quantum Mechanics, Vol. 3 [in Russian], Fizmatgiz, Moscow (1963).
22. A. Bohr and B. Mottelson, Kgl. Danske Vid. Selskab., Mat.-Fys. Medd., 27, N16 (1953).
23. J. Rainwater, Phys. Rev., 79, 432 (1950).
24. A. E. S. Green, K. Lee, and R. J. Berkley, Phys. Rev., 104, 1625 (1956).
25. J. W. Negele, Phys. Rev., C1, 1260 (1970).
26. S. Bjornholm and V. M. Strutinsky, Nucl. Phys., A136, 1 (1969).
27. D. F. Lazutkin, Zh. Vychislit. Matem. i Matem. Fiz., 10, No. 2, 362-373 (1970).
28. R. Balian and C. Bloch, Ann. Phys., 60, 401 (1970).
29. A. S. Tyapin, Yad. Fiz., 14, 88 (1971).
30. W. Kohn and L. J. Sham, Phys. Rev., A137, 1697 (1965).

31. P. J. Siemens, Phys. Rev., C1, 98 (1970).
32. V. M. Strutinsky and A. S. Tyapin, Zh. Eksp. Teor. Fiz., 45, 960 (1963) [Sov. Phys.—JETP, 18, 664 (1964)].
33. P. A. Seeger, Proc. of the Third International Conference on Atomic Masses, Winnipeg (1967).
34. V. M. Strutinsky, Proc. Int. Symp., "Why and How...," Lysekil, Sweden (1966), Almquist and Wiksell, Stockholm (1968), p. 629.
35. S. G. Nilsson, S. G. Thompson, and C. F. Tsang, Phys. Lett., 28B, 458 (1969).